Pericytes in Hypoxia and Ischemic Stroke

Enström, Andreas

2023

Document Version:
Publisher's PDF, also known as Version of record

Pericytes in Hypoxia and Ischemic Stroke

ANDREAS ENSTRÖM
DEPARTMENT OF CLINICAL SCIENCES | FACULTY OF MEDICINE | LUND UNIVERSITY

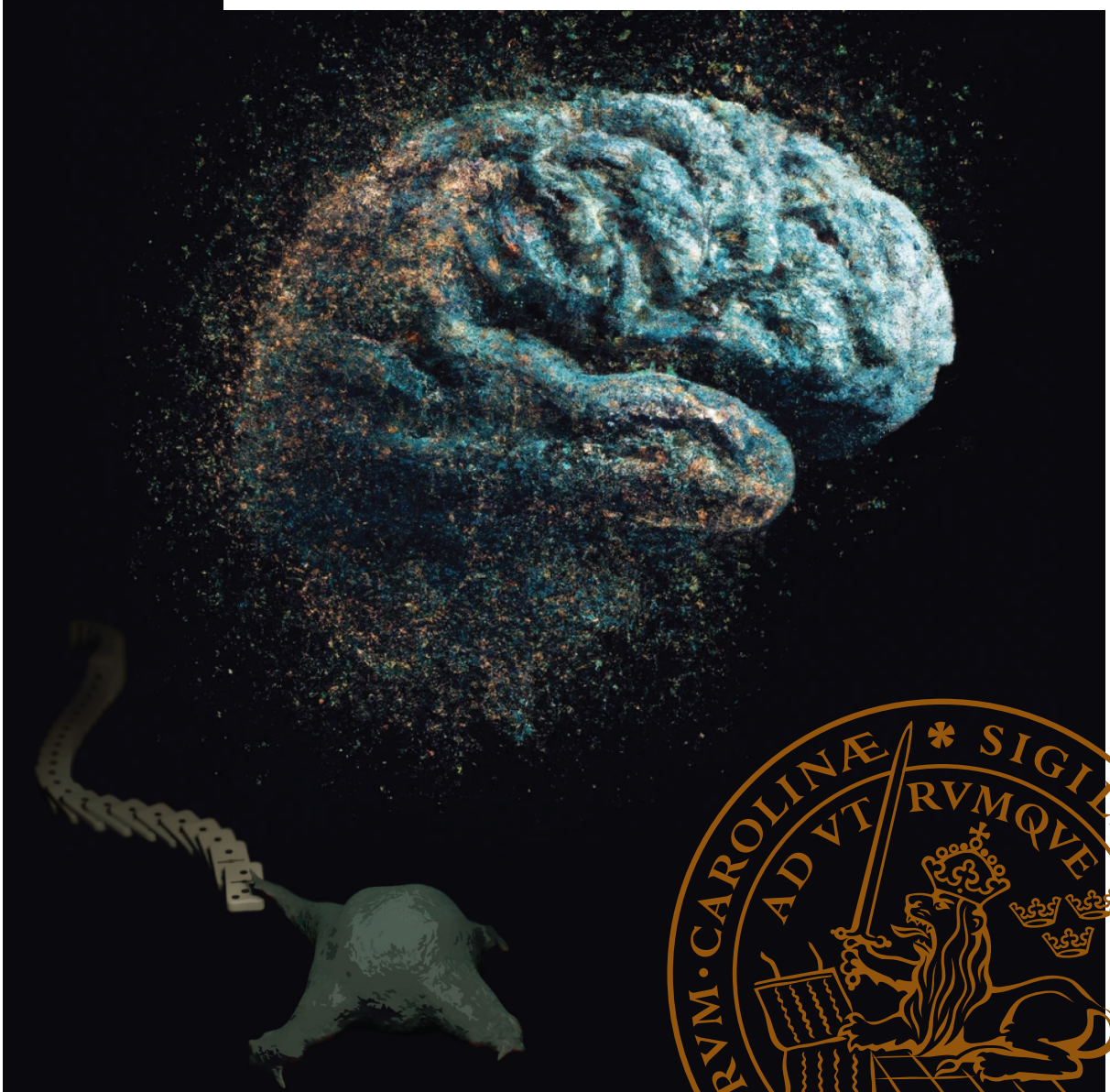

Pericytes in Hypoxia and Ischemic Stroke

Pericytes in Hypoxia and Ischemic Stroke

Andreas Enström

LUND
UNIVERSITY

DOCTORAL DISSERTATION

Doctoral dissertation for the degree of Doctor of Philosophy (PhD) at the Faculty of Medicine at Lund University to be publicly defended on 11th of May 2023 at 09.00 in Segerfalksalen, Sölvegatan 17, Lund, Sweden.

Faculty opponent
Associate Professor Axel Montagne

University of Edinburgh

Organization LUND UNIVERSITY Faculty of Medicine Department of Clinical Sciences Translational Neurology Group	**Document name** Doctoral Thesis **Date of issue** May 11, 2023
Author: Andreas Enström	**Sponsoring organization** Lund University

Title: Pericytes in Hypoxia and Ischemic Stroke

Abstract

Molecular oxygen is essential for most living species. Consequently, hypoxic or ischemic conditions are major cellular stressors and prominent pathological features in ischemic stroke. Stroke is a global health problem and remains the second leading cause of death or disability worldwide. Current management of the disease focuses on rapid reperfusion by thrombolysis or thrombectomy but these therapies are time-critical and only administered to a minority of patients. Thus, improving our understanding of stroke pathogenesis is key to ensure rapid and accurate diagnostics to maximize benefits from existing reperfusion treatments but also to identify new therapeutic targets. Blood-brain barrier (BBB) breakdown is one of the pathological hallmarks of ischemic stroke, excerbating the ichemic brain injury and limiting the use of current clinical therapies. Ischemic stroke is also characterized by endogenous repair mechanisms such as angiogenesis to restore cerbral blood flow, and neurogenesis for functional recovery. Understanding when and how the brain transitions from injury to repair and how the responses of specific cells may orchestrate that transition could have key implications for future stroke therapies.

Brain pericytes, surounding capillaries at the blood–brain interface have received increased attention in stroke research as they have central roles in maintaining BBB integrity, regulating angiogenesis, and modulating inflammation. As such, pericyte dysfunction after ischemic injury may have an unfavourable impact on BBB breakdown due to pericyte detachment and/or disruption of blood-flow because of pericyte constriction. On the other hand, pericytes in the peri-infarct area supports poststroke recovery by inducing angiogenesis and neurogenesis. However, we still have limited knowledge of how pericytes sense and respond to hypoxic/ischemic insult and further insght are needed. Towards that end, this thesis has aimed at expanding the current knowledge of the role of pericytes in the hypoxia or ischemia challenged brain from different perspectives.

One of the first pericyte responses to hypoxia or ischemia is the rapid induction of Regulator of G-protein Signalling 5 (RGS5), a negative regulator of G-protein signalling. Using an experimental mouse model of ischemic stroke we established that loss of RGS5 preserved the perivascular coverage of pericytes associated with increased vascular density and BBB integrity. In cell cultures of human brain pericytes, we show that RGS5 expression desensitizes pericytes to important chemotactic cues such as platelet-derived growth factor (PDGFBB) necessary for pericyte recruitment and retention to the vascular wall.

Pericytes secrete various factors important for cell-cell communication. Using an *in vitro* BBB-model, we show that the pericyte secretome is altered under hypoxia and dependent on cell-cell interactions of other BBB-residing cells. Furthermore, circulating pericyte-derived microvesicles (MVs) showed an early and time-dependent increase in stroke patients, where functional annotation of secreted molecules within the MV cargo related to inflammation and vascular remodelling.

Using single-cell RNA sequencing in an ischemic stroke mouse model, we identified a stroke-specific subcluster of pericytes present at different time points of the acute phase, characterized by the upregulation of specific genes related to cytokine signalling and modulation of the immune and inflammatory response.

Key words: Stroke, blood-brain barrier, pericytes, RGS5, secretome, transcriptome

Classification system and/or index terms (if any)

Supplementary bibliographical information Lund University, Faculty of Medicine Doctoral Dissertation Series 2023:62	**Language:** English
ISSN and key title: 1652-8220	**ISBN:** 978-91-8021-402-5

Recipient's notes	**Number of pages** 80	Price
	Security classification	

Signature 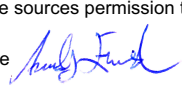 Date 2023-03-27

Pericytes in Hypoxia and Ischemic Stroke

Andreas Enström

LUND
UNIVERSITY

2023

Cover art by Andreas Enström

The front is an abstract depiction of ischemic stroke with pericytes at the top of the ischemic cascade. The back represents the vascular network of the brain with enwrapping green pericytes.

Faculty of Medicine
Department of Clinical Sciences

ISBN 978-91-8021-402-5
ISSN 1652-8220
Lund University, Faculty of Medicine Doctoral Dissertation Series 2023:62

Printed in Sweden by Media-Tryck, Lund University
Lund 2023

To my family

"The first principle is that you must not fool yourself – and you are the easiest person to fool."

-Richard Feynman

Table of Contents

Original Papers

Papers Included in This Thesis

Paper I

Regulator of G-protein signalling 5 regulates the shift from perivascular to parenchymal pericytes in the chronic phase after stroke.

Roth M., Gaceb A., **Enström A**., Padel T., Genove' G., Ozen I., and Paul G.

FASEB J (2019) 33, 8990-8998

Paper II

RGS5: a novel role as a hypoxia-responsive protein that suppresses chemokinetic and chemotactic migration in brain pericytes.

Enström A., Carlsson R., Ozen I., and Paul G.

Biol Open (2022) 11(10): bio059371

Paper III

Pericyte-specific secretome profiling in hypoxia using TurboID in an *in vitro* blood-brain barrier model.

Enström A., Carlsson R., Buizza C., Lewi M., and Paul G.

Manuscript in preparation

Paper IV

Pericyte-derived microvesicles as plasma biomarkers reflecting brain microvascular signalling at different stages of acute ischemic stroke.

Gaceb A., Roupe L., **Enström A**., Almasoudi W., Carlsson R., Lindgren A., and Paul G.

Manuscript in preparation

Paper V

The transcriptional landscape of pericytes in acute ischemic stroke

Buizza C., **Enström A**., Carlsson R., and Paul G.

Manuscript in preparation

Papers Not Included in This Thesis

Parenchymal pericytes are not the major contributor of extracellular matrix in the fibrotic scar after stroke in male mice.

Roth M., **Enström A**., Aghabeick C., Carlsson R., Genove' G., and Paul G.

Journal of Neuroscience Research 2019 November doi:10.1002/jnr.24557

Review

Molecular Regulation of the Response of Brain Pericytes to Hypoxia

Carlsson R., **Enström A**., and Paul G.

Int. J. Mol. Sci. 2023, 24(6), 5671 doi:10.3390/ijms24065671

Lay Summary

Stroke, also known as 'ischemic brain attack', is a medical emergency caused by a blood clot that prevents a certain brain region from receiving oxygen and nutrients. As a result, affected brain cells start to die within minutes and the injury progresses for several weeks. Current treatments are aimed at restoring blood flow by clot dissolving drugs but can only be administered within the first few hours after stroke onset. Therefore, there is a great need to find new therapies to slow down the disease progression or reduce the impact of the brain injury after stroke.

To develop effective treatments for stroke, it is important to have a comprehensive understanding of the molecular events that occur at the interface between the blood vessels and the brain. A key feature of stroke is the breakdown of the so-called blood-brain barrier. This breakdown leads to the leakage of blood vessels, swelling, and brain inflammation, all of which contribute to the severity of stroke.

Pericytes are cells that surround the blood-brain barrier and have important functions in the brain, such as maintaining blood-brain barrier functionality, initiating new blood vessel formation, and communicating with other brain cells. However, during stroke, pericytes change their behaviour by dropping off the blood vessels and altering their ways of communication which have a large impact on the pathological progression.

The work of this thesis has focused on expanding current knowledge of specific responses of pericytes after stroke and has attempted to identify novel targets that modifies pericyte behaviour to improve stroke outcome. Towards that end, we identified a gene known as *RGS5*, unique to pericytes in the brain that allows them to sense fluctuations in oxygen. In addition, mice lacking *RGS5*, had increased numbers of pericytes surrounding blood vessels, which was associated with protection of the blood-brain barrier after stroke.

After stroke, pericytes release a mixture of signalling molecules called the 'pericyte secretome'. This secretome may have both negative and positive effects in the brain. While it can help repair damaged tissue and promote new blood vessel formation, it can also contribute to inflammation and worsening of the brain damage. To better understand its effect, we developed a technique to extract the pericyte secretome from a cell-culture model of the blood-brain barrier. From that, we found that pericytes modify their secretome in conditions of low oxygen that may regulate important mechanisms such as blood vessel formation and cell metabolism.

Furthermore, examining blood samples from stroke patients, we detected an early increase of released signalling molecules originating from pericytes which also supports that the pericyte secretome is important for stroke recovery.

Finally, we employed a mouse model to investigate the gene expression profiles of individual pericytes after stroke. As stroke may provoke specific responses in different cell types as well as in subsets of the same kind of cell type, this type of analysis enables a comprehensive overview of the pathology. Through our analysis, we uncovered distinct subpopulations of pericytes that exhibited a time-dependent activation of specific genes in response to stroke, associated to brain inflammation.

Populärvetenskaplig sammanfattning

Stroke, aven känt som ’hjärninfarkt’, är ett akut medicinskt tillstånd som orsakas av en plötslig blodpropp som hindrar en del av hjärnan från att få tillräckligt med syre och näring. Till följd av detta dör de mest drabbade hjärncellerna inom några minuter, men skadan fortskrider under flera veckors tid. De nuvarande behandlingarna fokuserar på att återställa blodflödet med hjälp av propplösande läkemedel, men som endast kan tillämpas inom de första timmarna efter att en stroke har inträffat. Det finns därför ett stort behov av att hitta nya behandlingar för att bromsa sjukdomsutvecklingen eller att minska effekterna av hjärnskadan efter stroke.

För att utveckla effektiva behandlingar mot stroke krävs en omfattande förståelse av de komplexa molekylära händelser som sker vid gränsen mellan blodkärlen och hjärnan. Ett särpräglat fenomen vid stroke är att den så kallade blod-hjärnbarriären bryts ner. Denna nedbrytning leder till läckande blodkärl, svullnad och inflammation, vilket alla bidrar till allvarlighetsgraden av stroke.

Pericyter är celler som omger blod-hjärnbarriären och har viktiga funktioner i hjärnan, så som att upprätthålla barriärens funktionalitet, initiera nybildning av blodkärl och kommunicera med andra hjärnceller för att upprätthålla en fysiologisk balans. Vid stroke ändrar dock pericyterna snabbt sitt beteende genom att lossna från blodkärlen samt modifierar sina kommunikationssignaler, vilket har stor påverkan på sjukdomsförloppet.

Denna avhandling har inriktats på att utöka den nuvarande kunskapen om pericyters specifika reaktioner efter stroke och har försökt identifiera specifika molekyler som kan reglera deras svar efter stroke. I detta syfte har vi identifierat en gen (*RGS5*), som är unikt uttryckt av pericyter i hjärnan och fungerar som en cellulär sensor för att känna av fluktuationer av syrekoncentrationer. Möss som saknar *RGS5* visade sig dessutom ha ett ökat antal pericyter runt blodkärlen, vilket var associerat med bevarandet av blod-hjärnbarriärens integritet efter stroke.

Vid stroke kommunicerar pericyter med andra celler genom att släppa ut en blandning av signalmolekyler som tillsammans bildar vad vi kallar ett sekretom. Detta sekretom kan ha både negativa och positiva effekter i hjärnan. Samtidigt som det kan bidra till att reparera skadad vävnad och främja nybildning av blodkärl kan det också bidra till inflammation och förvärrande av hjärnskadan. För att bättre förstå effekten av detta, har vi utvecklat en teknik for att extrahera pericyters

signalmolekyler i en cellkultursmodell av blod-hjärnbarriären. Utifrån detta fann vi att pericyter snabbt modifierar sitt sekretom under syrefattiga förhållanden som kan reglera viktiga mekanismer som blodkärlsbildning och cellers metabolism. När vi analyserade blodprover från strokepatienter i en annan studie såg vi en tidig ökning av frigjorda signalmolekyler från pericyter vilket också stödde att pericyternas sekretom är viktigt för återhämtningen efter stroke. Slutligen använde vi en musmodell för att studera förändringar i genuttryck hos enskilda pericyter i hjärnan efter stroke, där vi identifierade unika populationer av pericyter, varpå särskilda gener aktiveras vid specifika tillfällen efter stroke som kan påverka sjukdomsförloppet, speciellt den inflammatoriska processen.

Abbreviations

Ang-1	Angiopoietin 1
ATE-1	Arginyl-tRNA transferase 1
ATP	Adenosine triphosphate
BBB	Blood-brain barrier
bFGF	Basic Fibroblast growth factor
CD11b	Integrin alpha M
DAMPs	Damage-associated molecular patterns
DEG	Differentially expressed genes
ECM	Extracellular matrix
ER	Endoplasmic reticulum
FACS	Fluorescence activated cell sorting
GDNF	Glial-derived neurotrophic factor
GFP	Green fluorescent protein
GPCR	G-protein coupled receptor
HIF	Hypoxia-inducible factor
IBA1	Ionized calcium binding adaptor molecule 1
IL	Interleukin
MetAP	Methionine aminopeptidase
MMP	Matrix metalloprotease
MVs	Microvesicles
NGF	Nerve growth factor
PBS	Phospho-buffered saline
PDCLX	Podocalyxin

PDGFBB	Platelet-derived growth factor BB
PDGFRβ	Platelet-derived growth factor receptor β
PDK1	Pyruvate dehydrogenase kinase 1
PFA	Paraformaldehyde
PHD	Prolyl hydroxylase domain
pMCAO	Permanent middle cerebral arterial occlusion
RGS5	Regulator of G-protein signalling 5
siRNA	Silencing RNA
TGF-β	Transforming growth factor β
tPA	Tissue plasminogen activator
VEGF-A	Vascular endothelial growth factor

Introduction

Oxygen: A Brief History

Oxygen is arguably one of the most important elements to sustain life and has likely played an important role in defining the biodiversity we see today. The combination of fossil and molecular records has allowed scientists to reconstruct major evolutionary events in earth's history (*1*). This has provided a relatively coherent timeline for the origin of different organisms and where they fit in the scientific tree of life (*2*). Nonetheless, decoding which environmental factors that were involved in the diversity and abundance of life is still being investigated (*2-4*). The rise of environmental oxygen levels and its role as a driver for the evolution and diversification of complex ´large life´, has received particular attention. While large life such as mammals that are dependent on oxygen appear abundant today, their appearance is still a late occurrence in the history of life. In fact, today and throughout earth's history, the dominant lifeforms are those of small unicellular organisms able to survive in reduced oxygen (hypoxic) environments (*5-7*).

The evolution of photosynthesis, which occurred around two billion years ago (*8, 9*) led to a drastic increase in surface oxygen levels, although geological records indicate that the oxygen concentration fluctuated substantially for a long period of time. Not until around five hundred million years ago where atmospheric oxygen levels stabilized at twenty-one percent did evolution of intracellular mechanisms allow the efficient utilization of oxygen, which has likely paved the way for complex multicellular life to evolve (*10-12*). The availability of oxygen facilitated new biochemical reactions by a specialized respiratory chain, since oxygen is particularly well suited as the terminal electron acceptor within mitochondria – the central energy-producing organelle (*13, 14*). This process is linked to a boost in intracellular adenosine triphosphate (ATP) production – the universal form of energy for all aerobic life forms. Beyond that, recent discoveries have established oxygen as the singular most common substrate across all known biochemical reactions (*15, 16*). Because of oxygen's high redox potential, it constitutes an ideal electron acceptor that is capturing energy for cellular use, but the utilization of oxygen also has a cost. The presence of oxygen introduces biotoxicity due to its high oxidizing properties where electron-transfer from biological molecules cause intracellular damage induced by reactive oxygen species (ROS) (*17, 18*). It has therefore been essential for aerobic life to evolve adequate defenses to control and

repair the damage induced by the inherent toxic properties of oxygen isoforms (*19, 20*). Thus, like with all biological systems, maintaining homeostasis is key to ensure continued survival, perhaps especially regarding oxygen concentrations. Although we humans and other metazoan species have evolved oxygen sensing mechanisms and adaptive homeostatic responses, large fluctuations in oxygen concentrations can exceed our adaptive capacity, leading to tissue and organ damage (*21, 22*). Not surprisingly, hypoxia is a major cellular stressor and a common pathological feature involved in some of the leading causes of death worldwide including stroke, ischemic heart disease, cancer, and other age-related neurodegenerative diseases (*23*). Despite oxygen's central role in evolution, physiology, and pathology we still lack a full understanding of how cells sense and respond to oxygen fluctuations and the consequences thereof.

Hypoxia

Almost all mammalian cell types (at least nucleated) can sense oxygen concentrations and have developed mechanisms of adaptation to a hostile environment such as hypoxia (*24*). Systemically, compensatory responses such as increased ventilation, higher cardiac output, and blood vessel dilation are common adaptive features to increase the supply of oxygen. On a cellular level, a multitude of responses follow, where selective suppression of ATP-consuming reactions, and altered metabolism are some of the canonical adaptations to ensure cell survival (*25*). Cellular hypoxia can be transient where these adaptive responses will discontinue once sufficient oxygen concentrations are restored. However, persistently reduced oxygen availability (chronic hypoxia), complicates the situation. Under such prolonged hypoxic conditions, chain-like reactions induce a cascade that alters gene expression and protein modifications that changes cellular behavior and could induce irreversible processes that may have detrimental effects and even cause long-lasting pathology (*26, 27*).

Cells can sense and respond to fluctuations in oxygen in two distinct ways; either by modifications of pre-existing proteins such as stabilization, phosphorylation, ubiquitination etc., or by transcriptionally inducing a hypoxia-mediated gene-regulatory network (*23*). The latter has received much attention since the discovery of hypoxia inducible factors (HIFs) for which Gregg L. Semenza, William G. Kaelin Jr, and Sir Peter J. Ratcliffe were jointly awarded the Nobel Prize in Physiology and Medicine in 2019. The identification of HIFs introduced a new paradigm and established a molecular framework for intracellular adaptation to hypoxia. Today, thousands of genes have been identified to be regulated directly or indirectly by HIF activation (*28*). HIFs are a family of α- and β-heterodimeric transcription factors, where HIF-1α is a key player in the hypoxic response. While the HIF-1β subunit is constitutively expressed, HIF-1α is rapidly degraded under normal oxygen

conditions (normoxia). The degradation is facilitated by oxygen sensing prolyl hydroxylases (PHDs) – enzymes that in the presence of oxygen, hydroxylates HIF-1α and primes it for ubiquitination and degradation (*29, 30*). As such, hypoxia inhibits PHDs enzymatic activity leading to the stabilization of HIFα's. HIF-1α dimerizes with HIF-1β to form a transcriptionally functional unit that translocate to the nucleus and bind to hypoxia response elements in the promoter region of genes regulating cell survival, angiogenesis, metabolism, erythropoiesis, and many other biological functions to maintain oxygen homeostasis (*31, 32*).

Common features of cellular adaptation to hypoxia are shown in (Fig. 1). One of the most prominent adaptations is the increase in cellular uptake of glucose and upregulation of glycolytic enzymes to facilitate anaerobic glycolysis. This is at least in part mediated by HIF-1α activation of target genes such as different glucose transporters (GLUT1 and GLUT3) (*33*). Beyond modifications in glucose metabolism, HIF-1α also shuts down the TCA-cycle by inhibiting pyruvate entry through upregulation of pyruvate dehydrogenase kinase 1 (PDK1), which instead leads to intracellular lactate accumulation (*34*). This initiates a cascade of secondary consequences as the reduced TCA-cycle turnover limits the availability of NADH and $FADH_2$, which are rate limiting reducing agents in the electron transport of the respiratory chain – leading to ATP depletion (*35*). In addition, dysregulation of electron transfer at the respiratory chain leads to induced ROS levels that may induce cellular apoptosis (*36*). Another consequence of diminished TCA-cycle activity is the reduced production of aspartate – an important molecule for nucleotide synthesis which results in reduced cell proliferation under hypoxia (*37*). Cells in hypoxia also display an altered secretome because of the cellular reprogramming and many of the induced secreted factors are directly downstream of important transcription factors such as HIFs (*38, 39*).

While the above-mentioned examples are part of the general hypoxic response that are canonically dependent on HIF-activation, many other cellular oxygen mechanisms extend far beyond the HIF pathway. Numerous other transcription factors that are rapidly activated under hypoxia have been previously described and also known to be critical for cellular adaptation (*40*). Beyond the alterations of the transcriptional landscape, changes in protein synthesis, stabilization and activation are also important mechanisms integrated in the hypoxic response. In fact, a recent study that performed a systematic assessment on cell survival identified 109 proteins

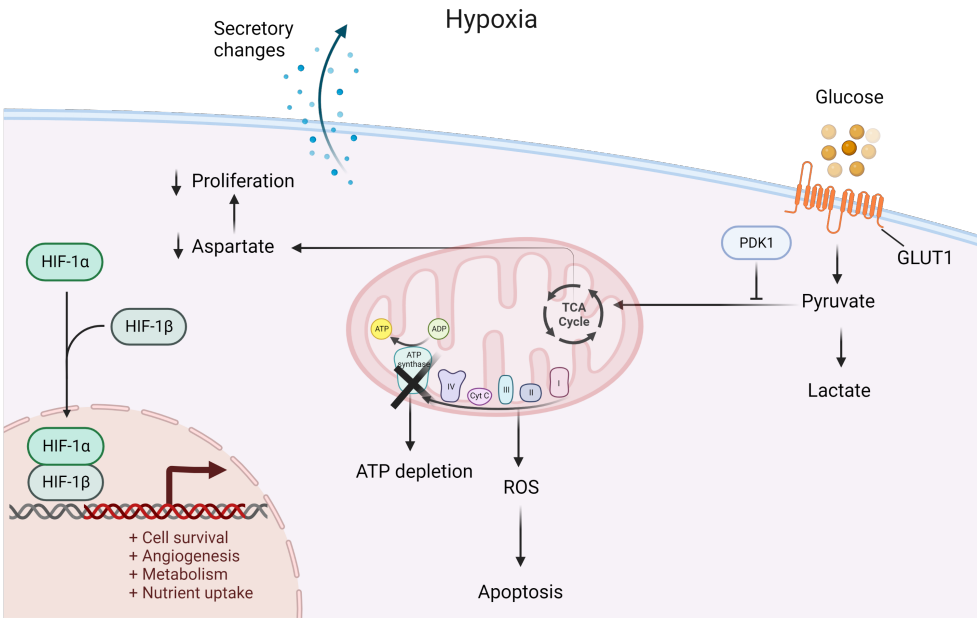

Figure 1. Overview of general cellular responses to hypoxic stress.
The figure highlights some of the general cellular responses to hypoxia correlated to HIF-activation. Hypoxic cells increase their glucose uptake to facilitate anaerobic glycolysis to ensure energy production as the mitochondrial metabolism is diminished due to reduced TCA-flux because of PDK1 inhibiting pyruvate entry which also leads to decreased ATP production from the respiratory chain. Respiratory chain dysfunction in hypoxia also leads to induced levels of ROS which may induce cellular apoptosis. Inhibition of the TCA-cycle also leads to depleted levels of aspartate which inhibits cell proliferation. Secreted factors important for intracellular communication have significant changes under hypoxia and may be important to coordinate an adeqauate response to hypoxic insult between cell types. Created in biorender.com

to be essential for survival under hypoxia, where most had no known regulation by HIFs (*41*). Despite many important discoveries over the last decades, we still lack a full understanding of which genes, proteins and pathways that are responsive to oxygen fluctuations and how they may differ depending on cell type and tissue. Future studies are warranted to increase our understanding of oxygen homeostasis and of clinically pathological conditions of hypoxia and ischemia.

Ischemic Stroke

Stroke is the second leading cause of death worldwide and one of the main reasons behind acquired adult disability (*42*). Stroke is a global problem, every 40 seconds someone is afflicted by stroke with an estimated death rate of approximately 42 percent. Among survivors, most stroke victims have compromised work capacity and around 30 percent require assistance with self-care. In the USA alone, stroke

was estimated to cost 73.7 billion dollars in 2010, and with an ageing population, these numbers are expected to increase more than 10-fold within the next 30 - 40 years (*43*). This acute neurovascular pathology is caused in the majority of cases (80 percent) by the occlusion of a blood vessel leading to brain ischemia, whereas the remaining (20 percent) are caused by intracerebral haemorrhage (*44*). In ischemic stroke – the sudden hypoxic insult and lack of nutrients such as glucose to the affected brain region amount to immense cellular stress and initiates a cascade of molecular events leading to cerebral ischemic injury and cell death (*45*). While some cell types appear to be more resilient to ischemia, neurons are especially vulnerable to ischemic injury due to their high dependence of oxygen and nutrient uptake (*46, 47*) and neurological dysfunction occurs within seconds to minutes after stroke onset. The complexity of stroke pathology is further characterized by a heterogenous response that progress throughout different phases for days, to weeks, up to months (*48*).

In the efforts of finding novel neuroprotectants, systematic meta-studies have shown that from over a thousand pre-clinical studies of potential neuroprotective candidates, only tissue plasminogen (tPA) has been translated into clinical practice (*49*). However, despite the high efficacy of tPA to restore blood flow to the brain, the treatment is only administered to a minority of patients as the risk of haemorrhagic transformation increases dramatically after 3 - 4.5 hours after stroke onset (*50*). The only other currently available treatment after stroke is mechanical thrombectomy which is also limited by a short time window of treatment and restricted to large vessel occlusions, only accounting for approximately 30 percent of all ischemic strokes (*51*). Thus, there is a great need to increase our understanding of stroke both for quick and efficient diagnostic purposes but also to develop new prophylactic and therapeutic strategies beyond the narrow time window of reperfusion strategies.

The Acute Phase of Ischemic Stroke

The brain is our most energy-demanding organ relative to its weight and consumes approximately 20 percent of the available oxygen at rest, to generate enough ATP to maintain full function (*52*). Stroke is therefore an acute condition where intracellular ATP depletion occurs within minutes as the ischemic injury introduces both hypoxic suppression of the respiratory chain, and the lack of supply of nutrients such as glucose that restricts anaerobic ATP synthesis by glycolysis. The first few hours of the ischemic injury correspond to the hyperacute phase of stroke, characterized by early cell death and blood-brain barrier (BBB) breakdown (*53*). The lack of ATP synthesis has rapid detrimental consequences in maintaining ionic gradients leading to intracellular influx of sodium causing plasma membrane depolarization. In addition, calcium pumps are also compromised, where the intracellular accumulation activates several death-signalling proteins such as

different proteases, lipases, and DNases, resulting in rapid cell death within the infarct core (*54*). In neurons, glutamate accumulation in the extracellular space because of ion pump failure and defective reuptake mechanisms leads to excitotoxicity, where prolonged activation of glutamate receptors enhances the influx of ions and water, which further accelerates cell death (*55*).

In ischemic stroke, the BBB breakdown is one of the main pathological features. The BBB is the multicellular microvascular network of the brain that actively regulates the transport of blood, ions, metabolites, and cells from the circulation to the brain and vice versa. Loss of the restrictive barrier capacity compromises this highly regulated exchange, leading to altered signalling homeostasis, and influx of immune cells and other blood-derived molecules into the central nervous system which further aggravates the pathology (*56, 57*) . The BBB breakdown is initiated by the ischemic injury and progressively increases with prolonged hypoperfusion due to lack of oxygen and nutrients (*58, 59*). While the exact timeline of BBB breakdown is still under debate, evidence supports it starting already within the first few hours after stroke onset (*60, 61*) and that increased permeability persists for several weeks in human patients (*62, 63*).

Another important aspect of acute ischemic stroke is the inflammatory response. The acute ischemia-induced cell death results in the release of damage-associated molecular patterns (DAMPs), that initiates a localized inflammatory response by activating vascular cells, microglia, and astrocytes to produce inflammatory cytokines and immune attracting chemokines (*64-66*). The BBB breakdown after ischemic stroke further enhances the inflammatory response by enabling infiltration of immune cells into the brain parenchyma. Such focal brain inflammation initiates a chain-like effect aggravating BBB damage, brain oedema, oxidative stress, and cell death (*67*). While the initial inflammatory response appear to amplify the ischemic injury, inflammation seems to have a biphasic role in promoting cellular secretion of beneficial neurotrophic factors and proangiogenic molecules necessary for the tissue repair at later stages of ischemic stroke (*45*).

The Chronic Phase of Ischemic Stroke

The ischemic injury results in two distinct areas defined as the stroke core and the peri-infarct area. Brain tissue within the ischemic core is often irreversibly damaged, even if reperfusion is restored. In contrast, the peri-infarct area that surrounds the infarct core is still challenged by ischemia, but less so, due to some compensation by collateral flow (*68, 69*). Thus, the peri-infarct area represents potentially salvageable tissue. However, as the ischemic injury progresses, the infarct core expands into the peri-infarct area, resulting in a defined window of opportunity to restore blood flow to the affected brain region. During the chronic phase of ischemic stroke starting days after ischemic injury, endogenous repair mechanisms such as angiogenesis, neurogenesis and scar formation takes place (*70, 71*).

Vascular remodelling is the brain's endogenous repair mechanism to restore cerebral blood flow (*72*). The hypoxic/ischemic insult leads to a surge in angiogenesis (the formation of new blood vessels). The angiogenic process in the infarct area may salvage some of the ischemic tissue but also sets the stage for functional reconstruction of neuron repair and regeneration that are dependent on sufficient oxygen and nutrient supply (*73, 74*). Typically, new vessel formations are observed within the first few days after stroke and continuously increase for several weeks (*75*). It is likely that modulating angiogenesis after stroke could have great benefits on stroke outcome. This is supported by previous post-mortem examinations of stroke patients showing increased microvascular density in the peri-infarct area, which correlated to increased survival rates (*76*). However, it is important to note that increased angiogenesis may induce a negative effect after stroke. The elevated and prolonged angiogenic response is connected to immature vessel formation that may lead to increased vascular permeability, oedema and neuroinflammation (*77, 78*). Therefore, the timing and spatial region of the angiogenic response after stroke are likely key factors in determining the tipping point of beneficial versus detrimental outcomes.

Like with any injury, wound healing is an important factor. The activation of astrocytes, microglia and other cell types after ischemic stroke seals off the necrotic tissue in the brain after ischemic stroke (glial scar). This physical barrier is further reinforced by structural extracellular matrix modifications of the infarct core that culminate into a permanent scar formation (fibrotic scar). Together, these processes enclose inflammatory cells within the core, preventing further brain inflammation. Whilst initial scar formation limits further brain damage, the scar has also been described to spread into viable regions of the brain and is widely believed to inhibit neuronal plasticity and repair mechanisms (*79, 80*).

Taken together, this brief description summarizes some of the general mechanisms of ischemic stroke pathology throughout its different phases. Yet, the complexity of this disease cannot be overstated. While many of the above-mentioned mechanisms have been studied in detail it is clear that we still lack enough information to efficiently address this global health problem. Thousands of promising pre-clinical therapeutic assessments have failed to translate into clinical application, and no new treatment has emerged since the FDA approval of tPA in 1996 (*81*). It is likely that for new efficient therapies to be discovered we must address the brain as a whole. This is becoming increasingly recognized as many of the detrimental and/or repair mechanisms during the pathological cascade of ischemic stroke are dependent on the intricate communication between the different cell types of the brain (*82*). Understanding how different cell types respond and how cellular communication affects the course of the ischemic injury will be important aspects for future research in stroke therapy. In ischemic stroke, the cells constituting the BBB, i.e., cells essential to maintain homeostasis within neurovascular niche, are the first to sense and respond to injury and set the stage for the pathological progression.

The Blood-brain Barrier

In 1885, the German scientist Paul Ehrlich injected water soluble dyes into the peripheral circulation of rabbits to estimate the oxygen consumption of different organs. To his surprise, the dyes did not stain the brain parenchyma, yet the other organs were permeated and heavily stained. The observations from these experiments led to the conclusion that the microvasculature in the brain must be equipped with a kind of barrier that restricts molecules from passing freely between the blood and brain (*83*). However, it was only several decades later that the first characterization of the unique barrier properties of the cerebral vasculature was described (*84*).

Today, the structure and function of the BBB has been well studied and is made up of the basement membrane, endothelial cells, pericytes and astrocytes. Endothelial cells of the BBB have distinct properties that distinguish them from peripheral vessels. The formation of specialized structures that connect and links endothelial cells together limits paracellular transport and transcytosis. An intact and fully functional BBB relies on pericytes that envelop the abluminal side of the endothelial vascular tubes, allowing direct crosstalk between the two cell types. Pericytes have key roles in BBB maintenance and integrity supported by several studies showing vascular dysfunction as a result of pericyte depletion (*56, 85*). Astrocytic endfeet (terminal processes of astrocytes) connect to endothelial cells and pericytes at the surface of the microvasculature and the distal neuronal synapses (*56, 86*). The BBB is highly dependent on dynamic communication between these cell types to maintain the BBB as well as construct coordinated responses when homeostasis is challenged. In addition to the different cell types of the BBB, the basement membrane consisting of several different extracellular matrix components, provides an anchor for vascular cells and the breakdown of the basement membrane is associated with increased BBB permeability (Fig. 2) (*87*).

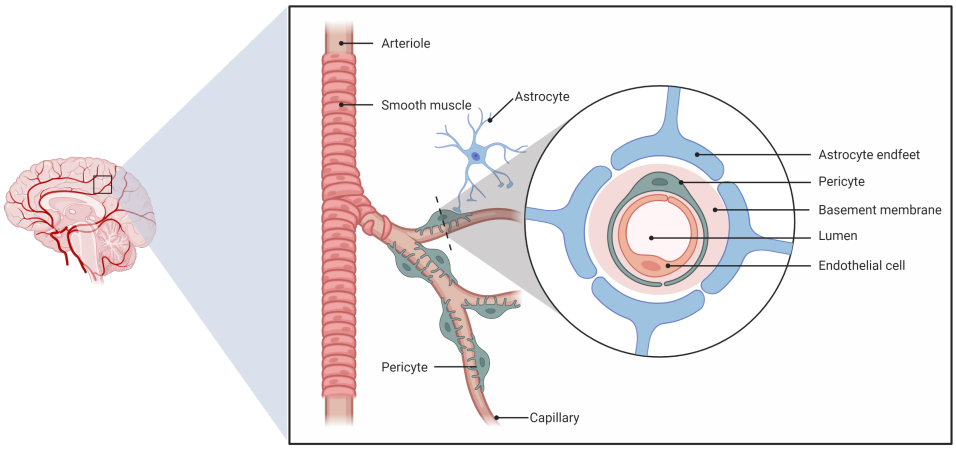

Figure 2. The Blood-brain barrier.
Brain penetrating arterioles surrounded by smooth muscle cells branches off into smaller vessels of the microvasculature, such as capillaries. These vessels consist of endothelial cells supported by enveloping pericytes and astrocytic endfeet that together with the basement mebrane form the highly selective blood-brain barrier. Created in biorender.com

Pericytes

A unique feature of the microvasculature and the BBB is the presence of pericytes. Large vessels such as arteries and veins consist of endothelial cells and a layer of smooth muscle cells, while smaller pre-capillary arterioles, capillaries, and post-capillary venules (known as the microvasculature) are instead covered by pericytes. Already in the late 19th century, Charles-Marie Benjamin Rouget made the first observation of branching cells that grip and envelop capillary blood vessels. However, it would take another 50 years before Karl Wilhelm Zimmerman coined the term pericyte referring to the cells (‘cyte’) positioned around (‘peri’) the capillary (*88*). In 1919, the Danish scientist August Krogh would disprove the then prevailing dogma that capillaries were passive vessels, but that they also regulate blood flow just as arterioles through dilation and contraction. Krogh was awarded the Nobel Prize for his discoveries the following year (*89*). Although unclear at the time, we now know that pericytes much like smooth muscle cells can contract and are responsible for the regulation of blood flow at the microvasculature. Since the discovery of pericytes, other attributes have been ascribed to this multifaceted cell type, and now we know that apart from contractility they have key roles in vascular stability, clearance, angiogenesis, extracellular matrix reorganization, inflammatory responses, and neurogenesis (*90*). However, some aspects of pericyte biology remain somewhat of a mystery.

Despite nearly 150 years of investigation, the definition and function of pericytes is still not clear. Lack of a specific marker facilitates an ongoing debate on the distinction between pericytes and smooth muscle cells (*91*). Another long-standing question is whether there are different subtypes of pericytes with unique features and functions. This hypothesis stems in part from the fact that certain brain pericytes are derived from the neural crest, while peripheral pericytes originate from the mesoderm (*92*). Isolated pericytes display multipotent stem cell abilities that rapidly differentiate into various lineages depending on the microenvironment stimuli (*93*). Further evidence of pericyte subtypes is their distinct morphology depending on microvascular location and developmental state (*91*). Thus, pericyte identification can be difficult and often require consideration of vascular location, morphology and an expression of different surface markers for an unambiguous identification which is not always applicable depending on the experimental setting (*94*).

Pericyte Function and Signalling

Over the last decades, many functions and signalling pathways have been assigned to pericytes. The following sections will describe some of the key aspects making pericytes an essential cell type of the brain's vascular network.

Angiogenesis

Pericytes have key functions during the highly regulated process of angiogenesis. Initially, proangiogenic stimuli such as hypoxia, stimulate pericyte release of matrix metalloproteases that degrades the basement membrane, remodels the extracellular matrix, and allow pericyte detachment from the vascular wall, necessary for sprouting endothelial tip cells to form (*95*). The pericyte release of proangiogenic factors, such as basic fibroblast growth factor (bFGF) and vascular endothelial growth factor (VEGF-A), stimulates endothelial cell proliferation and migration until new immature vascular tubes are formed (*96, 97*). To ensure vascular maturation and stabilization, pericytes then responds to chemotactic cues mediated by platelet-derived growth factor (PDGFBB) being secreted form endothelial cells, initiating pericyte migration and recruitment to the vascular wall (*98*). Specifically, endothelial-secreted PDGFBB stays bound to the surrounding extracellular matrix through its C-terminal retention motif forming a concentration gradient along the endothelial tip and stalk cells, ensuring the attraction of platelet/derived growth factor receptor (PDGFRβ)-expressing pericytes (*99*). Deletion of the PDGFBB retention motif does not only impair pericyte recruitment or proper vascular formation but has also been shown to impose pericyte detachment, illustrating the PDGFBB/PDGFRβ- signalling pathway to be essential for pericyte retention (*100*).

BBB maintenance and integrity

The human brain is our best perfused organ consisting of roughly 100 billion capillaries forming over a 650-kilometre-long vascular network (*101*). Capillaries of the central nervous system also have the highest ratio of pericytes in relation to endothelial cells (1:1 – 1:3), compared to e.g., the vasculature of skeletal muscle having only (1:100), indicating the important role of pericytes in maintaining barrier properties (*102*).

The closest neighbouring cell to pericytes are endothelial cells and their reciprocal communication is essential for BBB function. Direct physical interaction between these cell types is facilitated by peg-socket junctions, where small pericyte protrusions penetrate the acceptor socket of endothelial cells. These contacts are believed to be a sign of vascular maturation as the physical contact appears to prevent endothelial cell proliferation and angiogenesis (*103*). Furthermore, endothelial cell contacts are essential for barrier integrity. Adherens junctions and adherens plaques are necessary molecules that provide endothelial cell stability and regulate the BBB permeability of larger plasma proteins. These adherens complexes also facilitate pericyte anchorage that assists in controlling the orientation and abundance of these junctional proteins (*104, 105*). Unique to the BBB, is the endothelial expression of tight junction proteins. In contrast to adherens junctions, these complexes regulate the passage of smaller molecules less than 800 Daltons (*106*). Like with adhesion junctions, endothelial cells lacking pericyte interactions have been associated with abnormal tight junction assembly and increased vascular permeability (*107*). The intimate communication between pericytes and endothelial cells is further characterized by gap junctions through connexin-43 channels, that allow direct exchange of ions, small molecules and nutrients (*108*). Besides the contacts with endothelial cells, pericytes contribute to the regulation of the extracellular matrix of the basement membrane. Pericyte release of proteases assist in the degradation of the basement membrane, but they also contribute to the deposition of extracellular matrix proteins such as collagen IV, fibronectin and laminin for the functional assembly of the basement membrane around newly formed vessels (*109*). In addition, pericytes participate in the maintenance and clearance of the BBB, where they endocytose perivascular debris, foreign proteins and toxic metabolites (*110, 111*).

The pericyte secretome

Besides the direct forms of communication mentioned earlier, cells need to establish proximal or distal communication to orchestrate coordinated responses by releasing various signalling molecules into the extracellular space. Collectively, these molecules are known as the secretome. It is becoming apparent that this type of communication is not only essential to maintain physiological status but also plays a large part in pathology and recovery. In fact, recent findings show that beneficial effects from stem cell transplantation after central nervous system injury are mainly due to their secreted factors rather than cell engraftment (*112, 113*).

Recently, pericytes have become increasingly recognized for their secretory properties and release a variety of different cytokines, growth factors and extracellular matrix components (*114*). For instance, even under basal physiological conditions, pericytes release VEGF-A, transforming growth factor (TGF-β), angiopoietin-1 (ANG-1) and collagen IV, important for angiogenesis and vascular maturation. In addition, immunomodulatory interleukins (IL) such as IL-1α, IL-10 and IL-6 and even neurotrophic factors including nerve growth factor (NGF) and glial cell-derived neurotrophic factor (GDNF) are released by pericytes under controlled physiological conditions (*115-117*). Not surprisingly, pathological stimuli alter the abundance and content of the pericyte secretome. Still, most of the previous studies describing the pericyte secretome in different contexts are derived from *in vitro* studies of pericyte monocultures, allowing controlled conditions where secreted factors can be assigned to its cellular origin (*115, 118*). However, pericytes within tissues and organs do not reside in isolation, it is therefore unlikely that previous data accurately reflects the pericyte-secretome profiles present *in vivo*. Notably, the pericyte secretome is not only restricted to soluble factors released during paracrine signalling – secreted extracellular vesicles such as microvesicles (MVs) are another active component in pericyte communication (*119*). MVs are a form of membrane budding vehicles that can transport bioactive molecules such as proteins, RNAs, and lipids to recipient target cells (*120*). These means of transport allow for endocrine signalling - long distance pericyte communication within the same or even different organs (*121*). Thus, the pericyte secretome likely has multiple implications in physiology as well as pathology, where our current understanding is limited. Further elucidation of the pericyte secretome would necessitate characterization of pericyte-specific factors in multicellular or *in vivo* environments to provide better insights into its contribution to homeostasis, disease, and repair mechanisms.

Pericytes in Hypoxia and Ischemic Stroke

Previous stroke research has revolved around a neuro-centric view. It is becoming increasingly clear that neuroprotection is impossible without microvascular protection or restoration. Accumulating evidence supports that pericytes play a critical role in ischemic stroke pathogenesis and pericytes are one of the first responders to hypoxia/ischemia – which sets the stage for the progression of the pathological cascade.

Pericyte Constriction: The 'No-Reflow' Phenomenon

Brain reperfusion shortly after ischemic stroke is one of the best predictions of improved recovery. However, dysfunction of the BBB may disrupt efficient blood

circulation despite recanalization or dissolving of the blood-clot (*122, 123*). After occlusion of cerebral blood vessels, swelling of endothelial cells and astrocytic end processes along with fibrin deposits and aggregated leukocytes contribute to the narrowing of capillaries (*124*). Relatively recent discoveries have also attributed pericyte dysfunction as a component of this impaired reperfusion sometimes referred to as the 'no-reflow' phenomenon. In fact, within a few hours of ischemia, pericytes contract and remain contracted, leading to the trapping of circulating cells and continued obstruction of the blood vessel even though the initial blood clot is removed. This constriction in a subpopulation of pericytes is induced by influx and intracellular calcium release, thereby enhancing the myosin light-chain phosphorylation and stimulating the actomyosin contractile apparatus (*125*). The situation is worsened by an irreversible constriction of capillaries caused by a retained contractile state in pericytes even after cell death (similar to rigor mortis) (*126*).

Pericytes and BBB Breakdown

The BBB breakdown is at least in part due to the increased expression of matrix metalloproteinases (MMPs), that can have detrimental effects on stroke pathogenesis. MMPs degrades extracellular matrix components of the basement membrane that surrounds the BBB, where it exerts many essential functions such as structural support, signal transduction and cell anchoring (*127*). Previous findings support that pericytes rapidly induce the release of MMPs which contributes to increased vascular leakage and BBB degradation within the first 2-3 hours after stroke (*128*). BBB dysfunction is further characterized by disruption of junctional proteins that are otherwise essential to maintain the barrier integrity. While ischemic injury is correlated to decreased expression of different junction proteins, the initial disruption likely stems from the increased release of MMPs and ROS leading to their gradual degradation (*129*). In addition, the early detachment of pericytes after stroke further aggravates the situation.

Pericyte Detachment in Ischemic Stroke

One of the initial responses of pericytes to ischemic stroke is the detachment from the vascular wall followed by the migration into the brain parenchyma. This has been shown in several animal models supporting that pericytes leave the endothelium within the first 2-3 hours after stroke (*130, 131*). Whether this pericyte-detachment has beneficial or detrimental consequences has been somewhat debated. While it is a necessary step in initiating angiogenesis (as described above) as part of a reparative mechanism, the lack of pericytes at the endothelium leads to enhanced BBB breakdown further exacerbating injury (*132*). However, since controlled angiogenesis happens much later, this response is likely not contributing to vascular

repair but may be a sign of pericyte dysfunction in response to the severe disturbance in tissue oxygenation after ischemic injury. While the consequence of ischemic injury resulting in pericyte detachment has been well established, the regulation of this process has remained unclear. A previous study observed that pericytes leaving the vessels after stroke expressed the protein regulator of G-protein signalling 5 (RGS5), suggesting a possible correlation between the two (*133*). However, little is still known about the role of RGS5 in stroke and whether it is a consequence or effect of pericyte detachment has not been shown.

RGS5: Regulation, Expression and Function

RGS5 is a cytoplasmic protein that regulates the activity of G-protein coupled receptors (GPCR) – the most abundant family of receptors in the human genome. RGS5 activates the intrinsic GTPase activity of the GPCR, thereby hydrolysing the bound GTP into GDP, facilitating the termination of GPCR-signalling (*134*). While the role of RGS5 in ischemic stroke and hypoxia has remained somewhat elusive, it is commonly used as a pericyte marker and several biochemical properties of RGS5 have previously been described (*135*). One of the intriguing aspects of RGS5 is that it is exclusively expressed by mural cells (pericytes and smooth muscle cells) in the human brain (*136, 137*). Previous findings also suggest that RGS5 expression is one of the first responses of pericytes in hypoxic environments (*133, 138*). This proposes RGS5 as possible pericyte-specific target to modulate their response during stroke pathogenesis.

As previously mentioned, many of the so far discovered adaptive mechanisms of hypoxia have been ascribed to HIFs. HIF-1α has also been suggested for the regulation of RGS5; however, this study used human umbilical vein endothelial cells forced to overexpress RGS5 and to date no HIF-1α binding sites has been identified at the RGS5 promoter region (*135, 139*). Instead, there is substantial evidence supporting that RGS5 accumulation in hypoxia is regulated post-translationally via the N-degron pathway. This ubiquitin dependent pathway regulates the half-life of proteins depending on the proteins N-terminal configuration – requiring a cysteine residue position 2 (Cys-2) acting as a degradation signal. The N-terminal destabilization is initiated by methionine aminopeptidases (MetAPs) cleaving of the methionine and exposing the Cys-2 residue. Under normoxic conditions the Cys-2 is then oxidized and subsequently arginylated by arginyl transferase-1 (ATE-1), which primes RGS5 for ubiquitination and degradation (Fig. 3) (*140-142*).

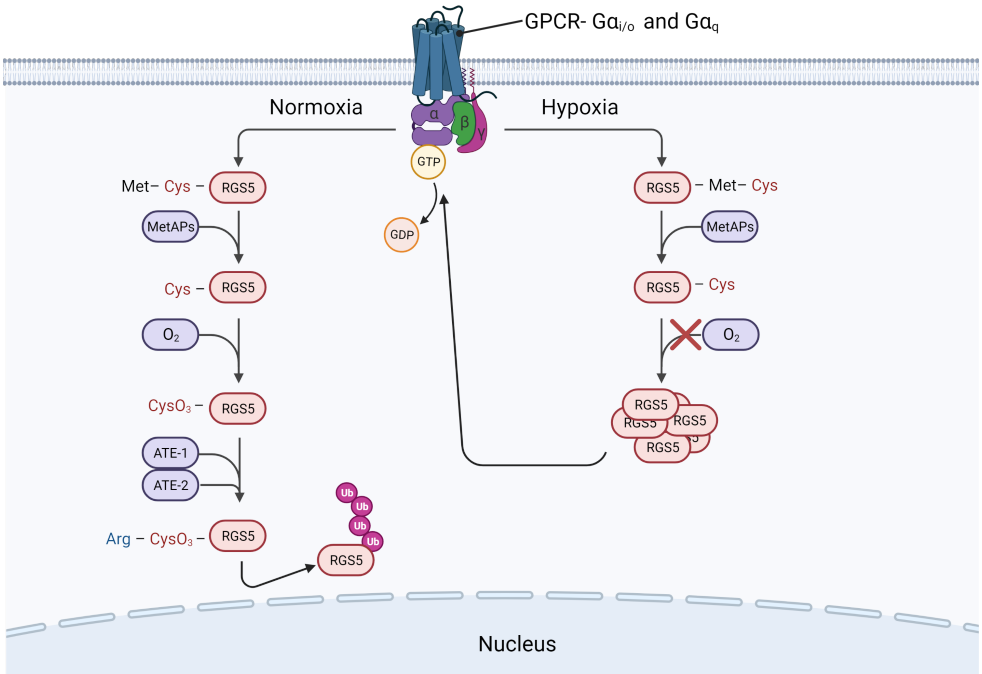

Figure 3. The degradation of RGS5 in normoxia by the N-degron pathway.
RGS5 is a substrate of the N-degron pathway due to its cysteine residue on position 2 (cys-2). Normoxic conditions allow the multi-step destabilization of RGS5. First the methionine on position 1 is cleaved by MetAPs exposing the Cys-2 residue. Next the Cys-2 residue is oxidized allowing arginine conjugation facilitated by ATE 1-2. This in turn primes RGS5 for ubiquitination and degradation. In contrast, destabilization of RGS5 is inhibited under hypoxia, leading to rapid intracellular accumulation where RGS5 inhibits GPCR-signalling. Created in biorender.com

Thus, even though RGS5 is constitutively transcribed, it has a very short half-life and low abundance in the presence of oxygen. Instead, it is likely that RGS5 has a role in the hypoxic response, whereby the Cys-2 oxidation is prevented, leading to rapid accumulation of intracellular RGS5. This response would allow quick inhibition of several signalling pathways in response to environmental stimuli like hypoxia or ischemia. The role of RGS5 in GPCR-signalling has been well studied, although there is still some uncertainty about which kind of GPCRs that RGS5 binds to. Previous studies suggest preferential binding to $G\alpha_{i/o}$ and $G\alpha_q$ and thereby exert control over several GPCR-agonists important for vascular control including sphingosine-1 phosphate, angiotensin II, and endothelin I (*137, 143, 144*). Yet, new non-GPCR targets of RGS5 are continuously being discovered and the molecular and physiological function of RGS5 in brain pericytes after stroke is not completely understood.

Fibrotic Scar

The glial scar has been well characterized both in rodent models and in humans after ischemic stroke involving hypertrophic astrocytes, activated microglia and macrophages that forms a border around the damaged brain region (*145, 146*). In contrast, less focus has been given to the non-glial fibrotic scar. After stroke the lesion introduces the influx of leukocytes and ECM-producing cells such as myofibroblasts. These cells are not cleared, nor replaced by regenerated tissue. Instead, they cluster together with the ECM-proteins in the infarct core and form the fibrotic scar (*147*). Previous studies have shown an increase in parenchymal PDGFRβ-expressing cells within the infarct core, suggested to contribute to the fibrotic scar by depositing collagen IV and fibronectin (*148, 149*). While PDGFRβ can be expressed by other cells than pericytes within the brain, it is possible that the detached parenchymal pericytes after ischemic stroke may participate in the fibrotic scar formation. In fact, scar formation in the central nervous system in mice after spinal cord injury or cortico-striatal lesions show that the major source of scar-forming fibroblasts originates from a specific subset of perivascular pericytes (*147*). However, little is still known of pericytes contribution to the fibrotic scar after ischemic stroke.

Pericyte Secretome in Ischemic Stroke

The pathogenesis of stroke has rapid detrimental consequences to the affected brain region. Unless perfusion is restored or cells made more resistant and capable of mounting an effective response to the ischemic injury, the tissue at risk deteriorates quickly (*150, 151*). The latter is getting increased attention in stroke research as the connection between cell-cell signalling is integrated into how each cell succumbs or adapts to hypoxic/ischemic injury (*152-154*). Understanding temporal changes in secreted factors from specific cell types after ischemic stroke will be important in defining mechanisms that may be beneficial or detrimental to identify new potential targets for future therapies.

Vascular cells like endothelial cells and pericytes are the initial sensors of ischemia or hypoxia. As ischemic injury likely induces perturbations in cellular communication, it is important to identify specific secretory changes that may drive or prevent disease progression (*45*). Hypoxic pericytes have been shown to increase the secretion of proangiogenic factors including bFGF, VEGF-A, TGF-β, and Ang-1, indicating important roles in vascular remodelling and repair (*114, 115, 155, 156*). Loss of trophic coupling between neurons and other cell types after ischemic stroke is likely a contributing factor in neuronal and glial vulnerability. Interestingly, *in vitro* studies show that hypoxic pericytes increase the release of NGF, BDNF, and, NT-4, possibly modulating neuronal plasticity and recovery (*157*). Pericytes also have immunoregulatory properties expressing DAMPs and toll-like receptors (*158*).

In vitro studies show that pericytes release multiple proinflammatory cytokines like IL-6, IL-8, IL-10, tumour necrosis factor-α and, IL-1β in response to various stimuli (*132, 159-161*). Further indication of pericytes immunomodulatory role is their phenotypic change after ischemic stroke where they start expressing microglial/macrophage markers such as galectin-3, ionized calcium-binding adapter-1 (IBA1), integrin alpha M (CD11b), and others (*133*). However, a full characterization of the pericyte secretome in response to hypoxia or ischemia is still lacking, especially in the context of more complex multi-cellular or *in vivo* environments.

Another understudied area is the secretion of pericyte-derived MVs in pathology. Only recently, a few studies have been conducted characterizing the contribution of pericyte-derived MVs in models of spinal cord injury and hypertension (*119, 162*). Since MVs are generated through budding of the plasma membrane, they also carry surface antigens, which allows them to be specifically traced back to their cellular origin (*163*). MVs can also pass the BBB and be detected in the peripheral circulation where they could serve as a plasma biomarker of pathology such as ischemic stroke (*164*). As such, MVs have great potential to contribute to existing diagnostic tools like magnetic resonance imaging, but analysis of the MV-cargo, will likely also reflect the severity and progression of the pathology that could help define new therapeutic strategies. Among vascular biomarkers in stroke, endothelial-derived MVs have been the most widely explored. A recent systematic review analysing results from five different studies in humans, reported elevated levels of circulating endothelial-derived MVs after ischemic stroke (*165*). However, a previous study also highlighted the inability to discriminate endothelial-derived MV-phenotypes between stroke mimics and stroke patients – perhaps limiting their use as stroke biomarkers (*166*). Considering pericytes early response and activation in response to ischemic stroke, together with their extensive secretory properties, future studies on pericyte-derived MVs could provide additional information on stroke and how pericytes respond during the pathological progression.

Pericyte Heterogeneity and Transcriptional Landscape

Studying stroke can be a challenging task due to the complex and varied multicellular responses the underlie the progression of the pathology. Additionally, the presence of various subtypes of different cell types (like pericytes), adds to the complexity of the subject. New techniques like single cell RNA-sequencing have already contributed to our understanding of cellular heterogeneity and it is likely that these advances will continue to increase our knowledge in this area (*167*). Transcriptional profiling has the possibility to provide important insights in the cellular composition and specific cellular responses to various pathologies. However, in stroke research, most previous transcriptome studies have been done using bulk-sequencing, which is unable to detect changes in gene expression from

different cell types or different cellular subtypes from the stroke region and mostly reflects the most abundant and susceptible cell types within the stroke region (*168, 169*). Other approaches such as analysing isolated cells or multicellular structures (e.g., microvessels) from the stroke-affected brain tissue, allow cell specific transcriptomic analysis but do not permit exploration of different transcriptomic patterns among other brain cells, and likely mask gene expression changes between cellular subtypes due to selection by specific marker expression (*170*). The few existing studies on stroke that utilized single cell RNA-sequencing, have mainly investigated the transcriptional response of neurons, astrocytes, and microglia but less attention has been given to pericytes (*171, 172*). This is partially because pericytes constitute a small cell population compared to other brain cells leading to difficulties in recovering enough cells for a comprehensive and reliable analysis. Despite that challenge, a recent study using a permanent stroke model in mice detected distinct subtypes of pericytes 24 hours after stroke onset, supporting a heterogenic response within the stroke region (*172*). Specifically, one subset of pericytes showed upregulated genes involved in potassium and calcium ion transport, membrane repolarization and regulation of PDGFRβ signalling – important to maintain BBB integrity. Other subsets of pericytes displayed expression of genes highly involved in oncostatin-M-induced BBB breakdown, inflammation, cytokine signalling, HIF-1α signalling, or extracellular matrix reorganization (*173*). In addition, a small subset of pericytes were also described to induce genes related to blood flow regulation and syndecan 1 pathway, known to promote cellular differentiation (*174*). These findings further support that the pericyte population is heterogenous, where subtypes may even have opposing effects after stroke onset, such as promote or prevent BBB breakdown.

Previous studies also support that the transcriptional landscape after stroke undergo drastic changes during the different phases of stroke progression where metabolic and inflammatory pathways are highly regulated in the early response while cell adhesion, ECM remodelling, and angiogenic pathways supervene at the early chronic phase (*169, 170*). A long-term temporal observation of the dynamic transcriptional changes will be key to assess the complete picture of specific cellular responses and their contribution to stroke pathogenesis.

Aims

I. In Paper I, we investigated if loss of RGS5 influences pericyte detachment, vascular density, and BBB integrity after ischemic stroke.

II. Here, we aimed at characterizing RGS5 regulation in hypoxia and determine its functional role - by assessing if RGS5 regulated pericyte migration, survival or proliferation in hypoxic environment.

III. In paper III, we aimed to characterize the pericyte secretome after hypoxic insult in co-culture conditions that resemble in vivo environments and using a method that allows to study the pericyte secretome specifically.

IV. Our aim was to explore if pericyte-derived microvesicles can be used as biomarkers and reflect the pathophysiology of the acute phase in human stroke patients.

V. Here, we aimed at characterizing the transcriptional landscape of pericytes and assess temporal changes in the acute phase of stroke that may have important impacts on progression of the pathology.

Key Methodology

The following section describes the key methods that have been applied during this thesis. For more detailed descriptions, protocols, and additional methods, see attached papers.

Animals

All animal experiments performed in this thesis were approved by the ethical committee of Lund University and conducted under the established guidelines and regulations. Animals were housed under standard conditions with a 12-hour light/dark cycle, with access to food and water *ad libitum*. Several different mouse strains were used, and experiments were conducted on male mice between 8-12 weeks of age. In **paper I**, we used a knock-out/knock-in *RGS5*$^{gfp/gfp}$ mouse strain, where green fluorescent protein (GFP) is expressed instead of RGS5 under the RGS5 promoter in a C57bl/6 background, referred to as RGS5-KO. As controls heterozygous *RGS5*$^{+/gfp}$ (referred to as RGS5-HET), and wild-type *RGS5*$^{+/+}$ (referred to as WT) were used. In **paper V**, RGS5-HET and WT mice were used. The rationale for using RGS5-HET mice was that it allows detection of RGS5-expressing pericytes based on GFP as it is still retaining RGS5 expression from one allele. Both in **Paper I and V**, RGS5-HET mice were utilized to track pericytes by histology or by flow cytometry, respectively.

In RGS5-KO mice, the genomic sequence of exons 2-5 has been replaced by a GFP cassette and have been thoroughly characterized showing no alterations in viability or fertility nor any obvious developmental or behavioural deficits (*175*).

pMCAO

Since the pathology of stroke has different underlying causes (ischemic or haemorrhagic) and outcomes depending on permanent vessel occlusion or restored blood-flow, several animal models of stroke exist. In this thesis (**paper I and V)**, we used a permanent model by inducing a middle cerebral arterial occlusion (pMCAO), characterized by high reproducibility, resulting in a localized stroke

lesion as previously described (*176*). Briefly, mice were anesthetized by isoflurane and marcain (AstraZeneca) was locally applied at the site of surgery for analgesia. A small incision (~ 1 cm) was made between the left eye and ear. The apical and dorsal part of the temporal muscle was detached and oved away from the skull, exposing the MCA in the rostral part of the temporal area. Using a surgical drill, a small craniotomy was made at the anterior distal bifurcation of the MCA, followed by arterial occlusion using electrocoagulation forceps (ICC50; Erbe), before the wound was sutured.

Tissue Collection and Cell Isolation

In **paper I**, mice were sacrificed at 7 days after ischemic stroke. Mice were perfused with phosphate-buffered saline (PBS), followed by 4% paraformaldehyde (PFA) before the brains were removed and fixed overnight. Subsequently the mice brains were incubated in 30% sucrose in PBS for 24 hours before sectioning. In **paper V**, mice were sacrificed at 1, 12, and 24 hours after ischemic stroke to evaluate the temporal transcriptional profile of acute ischemic stroke. Mice were perfused with 0.9% saline solution and brains were placed in saline solution on wet ice. Brains for histological analysis were fresh frozen and stored at -80 °C. Brains for cell isolation were kept on ice and the cortical part of the ipsilateral stroke region (ischemic core and peri-infarct area) was dissected. As control the same region for the contralateral cortex was also dissected. Subsequently, non-neuronal cells were isolated according to a previously published protocol (*177*). Briefly, the brain tissue was minced and dissociated by enzymatic digestion using collagenase IV (400 U/ml, Worthington Biochemical, Lakewood, NJ), dispase (1.2 U/ml, Worthington Biochemical Lakewood, NJ) and DNAse I (32 U/ml, Thermo Fischer Scientific). To remove neuronal myelin cells were resuspended in ice cold 20 % bovine-serum albumin (BSA) and centrifuged at 1,000 x g for 25 minutes, before resuspension in PBS supplemented with 0.5% BSA.

Histology and Immunocytochemistry

Histological preparations have varied slightly between studies. In **paper I**, PFA-fixed coronal free-floating sections in 12 series at 40 μm thickness were used compared to **paper V,** coronal sections of fresh-frozen brains were cut on the cryostat at 20 μm thickness and postfixed with 4% PFA on glass slides. Immunohistochemistry was performed using standard protocols (see full method sections in respective papers).

For immunocytochemistry in **paper III**, monocultures of human brain vascular pericytes (HBVP, ScienCell) were seeded on coverslips coated with fibronectin (1 µg/ml) and fixed with 2% PFA for 20 minutes. Spheroids were fixed with 2% PFA for 30 min and washed with PBS before being embedded in optimal cutting solution (OCT) and cryo-sectioned at 16 µm. The fixed cells or spheroids were blocked in 5% donkey serum diluted in 0.3% PBS-T for 1 hour before primary antibodies incubation in blocking solution overnight at 4 °C. Correlating secondary antibodies were incubated for 1 hour at room temperature and nuclear stain was obtained using DAPI. Fluorescent imaging acquisition from **paper I, III and V**, were obtained by either a Lecia SP8 or DMi8 confocal microscope.

BBB Leakage

Briefly, BBB breakdown and leakage were assessed by injecting 0.1 ml of 2% Evans blue into the tail vein 2 hours before the mice were perfused. Evans blue binds with high affinity to serum albumin with a molecular weight of 67 kDa and exhibits long blood half-life making it a good predictor of increased vascular permeability (*178*). For further details see method section in **paper I.**

Cell Culture

Different cell lines have been used for the *in vitro* studies conducted in this thesis. In **paper II**, we used primary HBVPs isolated from cortex tissue (Cell-systems). The HBVPs were maintained in complete classic medium (Cell-system) supplemented with 10% serum, 5 ml of CultureBoost and 2 ng/ml of Bac-off and seeded in culture plates coated attachment factor (Cell-systems). For **paper III**, HBVPs from ScienCell were seeded on 0.1% gelatine coated plates and cultured in pericyte medium (PM, ScienCell), supplemented with 2% serum, 100 µg/ml of penicillin/streptomycin, and growth factor supplement supplied by the manufacturer. In addition, human brain microvascular endothelial cells (HBMEC, ScienCell) seeded on 0.1% gelatine plates were maintained in in endothelial cell medium MV2 with 5% serum (ECM, PromoCell), and human primary hippocampal astrocytes (HAsc) seeded on 1 µg/ml fibronectin coated plates were cultured in Advanced Dulbecco's Modified Eagle Medium (DMEM F12, Gibco), supplemented with 10% serum and 100 µg/ml P/S. Co-culture spheroids were generated by combining HBVP, HBMEC, and HAsc in a 1:1:1 ratio of 10,000 cells of each cell type. To prevent cell attachment and allow spheroid formation the cell suspension was seeded in 96-well plates coated with 1% agarose and maintained in medium generated by mixing PM, MV2 and astrocyte medium in a 1:1:1 ratio.

Generation of TurboID-expressing Pericytes

To label the pericyte secretome, we generated a stable pericyte cell-line expressing the biotin ligase TurboID, using lentiviral transduction. Lentivirus was prepared in HEK293 cells maintained in DMEM supplemented with 10% serum and 100 µg/ml P/S before transfected at 80% confluency. The HEK293 cells were transfected with the lentiviral vector TurboID-V5 pLX304 (1573 ng), envelope plasmid pMD2.G (397 ng), and packaging plasmid pBR8.1 (849 ng) using lipofectamine 2000 (Thermo Fischer Scientific). Six hours after transfection the medium was changed to normal pericyte medium. Next, the virus was harvested at 48 and 72 hours after transfection and filtered through a 0.45 µm filter. Subsequently, HBVPs were transduced with 1.5 ml of the virus titre and cultured for 24 hours before expansion in selection medium containing 4 µg/ml of blasticidin, replacing the medium every 3 days for two weeks.

Hypoxia *in vitro*

Hypoxic Induction

To achieve a hypoxic environment, utilized in **paper II and III**, cells were transferred to a humidified gas-tight hypoxia chamber (Electrotek) with a gas composition of (85% N_2, 10% H_2, and 5% CO_2) generating an oxygen supply between ~ 0.5-1%. For consistency, the cell medium used in hypoxic experiments was pre-bubbled with N_2 gas for 15 minutes for deoxygenation before being applied to the cells. To monitor the hypoxic environment, an anaerobic indicator solution (Electrotek) with a threshold of less than ~ 1% oxygen was used containing (2% w/v $C_6H_{12}O_6$, 9% w/v $NaHCO_3$, and 1% w/v methylene blue solution).

Hypoxic Live-imaging and Analysis

For hypoxic live-imaging to assess pericyte chemotaxis, pericytes were seeded on fibronectin (10 µg/ml)-coated chemotaxis µ-slides and left to adhere overnight. Next, pericytes were transferred to the hypoxic chamber and the media was exchanged to deoxygenated N_2 pre-bubbled media. Next, PDGFBB (50 ng/ml) or S1P (1 µM) was applied to the left chamber of the µ-slide forming a concentration gradient to evaluate their chemotactic properties. The µ-slides were incubated for 1 hour in the hypoxic chamber before they were transferred and imaged using a Cell Discoverer microscope (Zeiss), with a humidified chamber at 37 °C and a hypoxic atmosphere with 0.1 % oxygen. Pericytes were imaged at 15-minute frame intervals for the duration of 22 hours using a 20x objective with 0.5x magnification. For imaging analysis, pericytes were tracked using the ImagJ plugin MtrackJ where the

x and *y* coordinates were extracted, computed and statistically analysed using the chemotaxis and migration tool 1.01 (Ibidi Integrated BioDiagnostics). All cell trajectories were extrapolated so that the $x, y = 0$ at the start point of time 0 hours of live-imaging.

RNA

Table 1. List of primers used in this thesis.

Paper	*Gene*	*Forward primer*	*Reverse primer*
II	*RGS5*	GGTCTTGGCTGGTTTCTCTG	GTGCAAAGGACTTGCAGCTT
II	*HIF-1α*	AGGGCAGGATACACANGATTTG	TTCCCGACTAGGCCCANTC
II	*S1PR1*	TCTGCGGGAAGGGAGTATGT	CGATGGCGAGGAGACTGAA
II	*S1PR2*	CGTTGGCATCAAAGATGGACA	CGATGGCGAGGAGACTGAA
II	*S1PR3*	TCTACCATCCTGCCCCTCTAC	ACACGCTCACCACAATCACC
II	*S1PR4*	CAACCCCATCATCTACTCCTTCC	AAAGCTGTCCCTTGGCCTC
II	*S1PR5*	TGTATTTATGCAGCGACACCCC	CTTCCCTGACCACCATCACC
V	*ADAMTS4*	CCCATTTCCCGCAGAACCAAG	CCTGCCGGGTGAACAGAATG
V	*RDH10*	CAGGCATGGTTCGCCACATC	CCTCACCTTTTCCAGCTTGCAG
V	*IL6*	CGTGGAAATGAGAAAAGAGTTGTGC	GGAGAGCATTGGAAATTGGGGT
V	*MT2*	TCTCGTCGATCTTCAACCGC	GCACTTGTCGGAAGCTCTT
V	*FSTL1*	GAAGCCTCTGTGTTGACGCC	TCCTCCAGGGCACACTTCTTC
V	*DBN1*	GTCGTCCGTACTGCCCTTTCA	AGTCTCCTGGGCCTCTTGAGT
V	*EDNRB*	CTGCGGAGGTGACCAAAGGA	TCCTCTGCGAGCAACTTGTAGG
V	*STC1*	TCGCCAATGGGATCACCTCC	CGGACAAGTCTGTTGTAGTATCTGT
V	*CCL2*	CTTCCTCCACCACCACCATGCG	AAGGCATCACAGTCCGAGTCA
II and V	*β2M*	CATTCCTGAAGCTGACAGCATTC	TGCTGGATGACGTGAGTAAACC

Quantitative Real-time qPCR

Total RNA was extracted using RNeasy plus Mini kit (Qiagen) according to the manufacturers protocol. Next, cDNA amplification was performed using Maxima First Strand Synthesis kit (Thermo Scientific) and Real-time qPCR samples were prepared using, Sso advanced Universal SYBR Green supermix (**paper II**) or PowerUp SYBRgreen Master Mix (**paper V**) (Thermo Scientific) and run on a CFX96 PCR-system (Bio-Rad). Primers used in this thesis are listed in (Table 1).

Single-cell Sequencing

In the preparation for single-cell RNA-sequencing, we used fluorescence-activated cell sorting (FACS). We first verified that our isolated cells contained sufficient numbers of live pericytes using RGS5-HET reporter mice positive for GFP. Pericyte validation was confirmed by ($CD140b^+$, $CD13^+$, GFP^+, $DAPI^-$, and $PECAM^-$). For transcriptomic analysis, we sorted 8,500 live-cells ($DAPI^-$), for each sample using

BD FACS Aria II flow cytometer system. Next, RNA was prepared for 10x reactions using the v3.1 3' x10 kit and cDNA libraries were amplified according to the manufacturer's instructions. Then, the single-cell libraries were sequenced on the Illumina NOVA-seg platform for samples analyse at 1 and 12 hours, and HiSeq-seq for the 24-hour samples after stroke. The genes were counted using the Cell ranger software version 5, and cell ranger aggr was used for sequence-depth normalization between each run. Next, the sequencing data was normalized using the Seurat suite version 4 and cells with a feature <200 or a mitochondrial gene content of >10% were filtered out. The data was log-normalized, before bioinformatic analysis.

Protein

Mass Spectrometry Preparation

In **paper III**, we used biotin-streptavidin pull downs for protein purification of the pericyte-specific secretome. Supernatant, harvested after 24 hours of hypoxia or normoxia were purified the same way for both monocultures and spheroid co-cultures. To eliminate streptavidin contamination and increase our sampling depth for proteomic analysis we chemically modified magnetic streptavidin beads making them resistant to proteolytic cleavage from proteases such as trypsin (Thermo Scientific), according to a previously published protocol (*179*). The streptavidin beads were then incubated with the cell culture supernatant (450 µl) containing biotinylated secreted proteins of pericyte origin and mixed with 450 µl of RIPA buffer and left rolling overnight at 4 °C. Next, we applied a protein enrichment protocol published previously (*180*). To eliminate non-biotinylated proteins beads were thoroughly washed twice with RIPA, once with 1M KCL, once with 0.1M Na_2CO_3, once with 2M Urea in 10 mM Tris-HCL, twice with RIPA, once with 50 mM Tris-HCL followed by 2 washes with 2M Urea in 50 mM Tris-HCL. For protein recovery by on-bead tryptic digestion, beads were incubated for 1 hour in 80 µl of 2M Urea in 50 mM Tris-HCL supplemented with 1 mM dithiothreitol (DTT) and 0.4 µg of sequencing grade trypsin (Promega) at 37 °C with shaking (1,000 rpm). Next, DTT was added to a final concentration of 4 mM to reduce the disulphide bonds before a final concentration of 10 mM of iodoacetamide used as an alkylating agent was added and incubated at 25 °C for 45 min in the dark. An additional 0.5 µg of trypsin was added to the samples before overnight digestion followed by desalting using C18 stage tips before running on the Exploris 480 mass spectrometer (Thermo Fischer Scientific) coupled with a Vanquish Neo Ultra-high performance liquid chromatography system.

Western Blot and Silverstaining

In **paper II and III**, western blotting constituted one of the key methods. Protein was denatured in Laemmli buffer (Bio-Rad) supplemented with 0.1 M DTT and boiled at 95 °C for 5 minutes. Samples were run on 15-well precast 4-15% SDS-PAGE gels (Bio-Rad) before transfer to nitrocellulose membranes (Bio-Rad). The membranes were blocked with 5% milk diluted in tris buffered saline supplemented with 0.1% Tween-20 (TBS-T), for 1 hour. Primary antibodies were suspended in 5% bovine serum albumin (BSA) diluted in TBS-T and incubated with the membranes overnight at 4 °C. Membranes were then washed and secondary horse radish peroxidase (HRP)-conjugated antibodies were diluted in 5% milk in TBS-T and incubated for 1 hour at room temperature. After washing, HRP substrates such as Clarity or Clarity Max (Bio-Rad) was used to measure chemiluminescence using a ChemiDoc XRS-system (Bio-Rad). All primary antibodies used for western blotting are listed in (Table 2). For visualization of biotinylated proteins in **paper III**, membranes were incubated directly with streptavidin-HRP conjugated antibodies diluted in 5% BSA in TBS-T directly after blocking. To visualize total protein, we applied silverstaining (Thermo Fischer Scientific), according to the manufacturer's protocol. Briefly, samples were prepared and run in the same way as for western blots. Gels were washed with MilliQ water before fixated in 30% ethanol and 10% acetic acid. Next the gel was washed with 10% ethanol and MilliQ water, then submerged in sensitizer solution and later stained with working solution for 30 min at room temperature. The gel was then developed for 2-3 minutes before adding the stop solution. Gels were imaged on the same ChemiDoc XRS-system. Western blotting was also performed in **paper I**, for further details, see attached paper.

Table 2. List of antibodies used for western blot in this thesis.

Paper	*Antibody*	*Species*	*Company*	*Cat. Number*	*Dilution*
II	RGS5	Rabbit	Protein Tech	11590-1-AP	1:1000
II	p-P44/42	Rabbit	CST	9101s	1:1000
II	P44/42	Rabbit	CST	9102s	1:1000
II	p-AKT	Rabbit	CST	9271s	1:1000
II	AKT	Rabbit	CST	9272s	1:1000
I and II	p-PDGFRβ (Y751)	Rabbit	CST	3161s	1:1000
II	p-PDGFRβ (Y1021)	Rabbit	CST	2227s	1:1000
I and II	PDGFRβ	Rabbit	CST	4564s	1:1000
II	HIF-1α	Rabbit	CST	36169s	1:1000
III	Anti-V5	Mouse	Thermo Scientific	R96025	1:400
III	Streptavidin-HRP	-	Southern Biotech	7100-05	1:50,000

Stroke Patients

Ethical Considerations

The study was approved by local ethical committees in accordance with the Declaration of Helsinki. Reporting guidelines according to Strengthening the Reporting of Observational Studies in Epidemiology (STROBE) was followed and samples and clinical data was acquired after written consent of the patient or authorized representative.

Plasma Sample Collection

Blood samples collected in EDTA tubes between 0-6 hours, 12-24 hours, or 2-6 days after stroke onset were placed on ice for a maximum of 2 hours. Next, the blood samples were centrifuged at 750 x g for 20 minutes at 4 °C and the plasma was extracted. Subsequently the plasma was centrifuged at 1,500 x g for another 20 minutes before the platelet-free plasma was stored at -80 °C, until further use.

MV Isolation and Phenotype Characterization

For MV isolation, platelet-free plasma was centrifuged at 21,000 x g for 45 minutes and supernatant was removed. MVs were then resuspended in 0.9% saline and stored at 4 °C. Pericyte-derived MVs were isolated based of PDGFRβ-expression using a CD140b-PE anti-human (Biolegend) and isotype-matched irrelevant human IgG served as a negative control. MV samples were then run on a BD FACS ARIA III flow cytometer.

Statistics

Statistics was performed using either IBM SPSS for two-tailed univariable linear regressions (**paper IV**) or using GraphPad prism. Normality testing was done when applicable. Nonparametric data were analysed by Mann-Whitney. Parametric data was analysed by unpaired Student's *t*-test and for multiple group comparisons one-way or two-way ANOVA with Tukey's multiple comparison, or multiple *t*-tests for specific group comparisons. P value ≤ 0.05 was considered significant.

Summary of Key Results

This section will summarize the key results from the respective papers presented in this thesis. For more details, see attached papers at the end of this thesis.

Paper I | Regulator of G-protein Signalling 5 Regulates the Shift from Perivascular to Parenchymal Pericytes in the Chronic Phase After Stroke

Previous studies have established RGS5 being exclusively expressed by activated mural cells in the adult brain after hypoxic/ischemic insult. Interestingly, RGS5-expressing pericytes are associated with pericyte detachment after ischemic stroke. However, whether RGS5 is the cause of this effect has not been shown (*133, 181*). To elucidate the role of RGS5, we used RGS5-KO, RGS5-HET, and WT mice to evaluate whether loss of RGS5 has an impact on pericyte detachment and pathological outcome after ischemic stroke, using a pMCAO stroke model.

Loss of RGS5 Results in Reduced Density of PDGFRβ-expressing Cells in the Infarct core

It has previously been established from several independent studies that the density of PDGFRβ-expressing cells progressively increases in the infarct core after ischemic stroke, likely contributing to the fibrotic scar formation (*133, 148, 182*). To assess whether RGS5 affected the morphology or density of PDGFRβ expressing cells, we compared WT and RGS5-KO mice 7 days after ischemic stroke. Examining the contralateral hemisphere, PDGFRβ-cells showed no obvious difference in density between genotypes and PDGFRβ expression was confined to cells with typical pericyte morphology. Within the infarct core, both WT and RGS5-KO mice displayed a densely packed area of PDFGRβ^{+} cells with atypical cellular protrusions and morphology (Fig. 4A). However, the quantitative analysis showed that RGS-KO mice had significantly lower density of PDGFRβ staining compared to the WT (Fig. 4B).

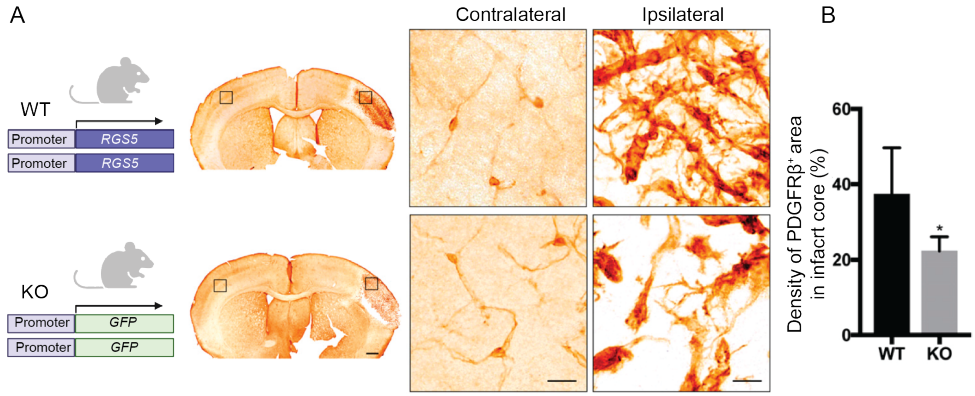

Figure 4. Lack of RGS5 results in reduced density of PDGFRβ-expressing cells within the infarct core.
A Representative bright field images of PDGFRβ-staining of WT or RGS5-KO mice, 7 days after ischemic stroke. Left panel illustrates genotype and overview images where the black boxes indicate the region of the magnified images displayed in the right panel. **B** Quantification of the PDGFRβ-staining in the infarct core. Data is presented as means ± S.D. Statistical testing was performed using Students *t*-test, n=6. Scale bars are 500 µm (overview) and 10 µm (magnified).

Loss of RGS5 Leads to Increased Numbers of Perivascular Pericytes

Next, we assessed whether RGS5 regulates the perivascular or parenchymal location of pericytes after stroke. Immunohistochemical evaluation 7 days after ischemic stroke revealed the RGS5-KO compared to RGS5-HET mice retained a 2-fold change higher pericyte coverage of the vascular wall in the infarct core, evident from the increase in the number of GFP^+ pericytes located around the podocalyxin (PDCLX)-positive capillaries. Importantly, pericytes in the infarct core of RGS5-KO animals were only found to have a perivascular rather than parenchymal location (Fig. 5A). Next, we assessed the relation between $PDGFR\beta^+$ and GFP^+ cells within the infarct core. Interestingly, only perivascular $PDGFR\beta^+$ cells expressed GFP. Quantification showed that the number of $PDGFR\beta^+/GFP^+$ pericytes was over 2-fold higher in the RGS5-KO mice, further supporting that lack of RGS5 results in increased perivascular location of pericytes, while RGS5-expressing pericytes likely detach and migrate into the parenchyma (Fig. 5B).

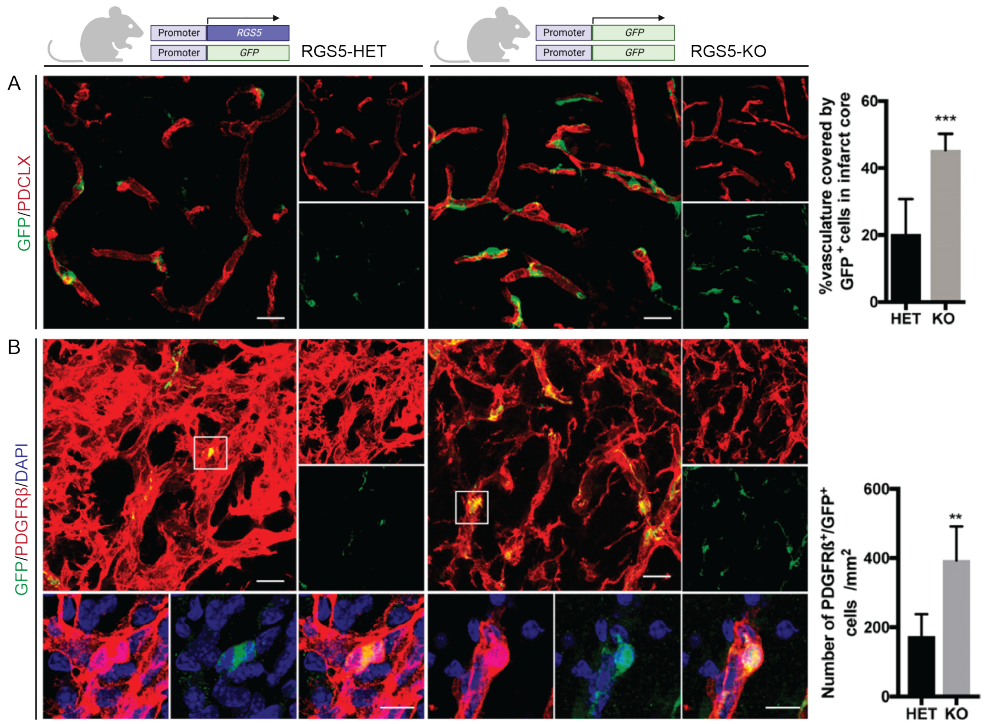

Figure 5. Loss of RGS5 leads to higher vascular coverage of pericytes 7 days after ischemic stroke.
A Representative confocal images of the infarct core after experimental ischemic stroke of GFP expressing pericytes in green and the vasculature in red stained for podocalyxin (PDCLX). The right panels of fluorescent images shows single channels of PDCLX and GFP, respectively. The quantification of the percentage of the vasculature covered by GFP expressing cells is shown to the far right. **B** Representative confocal images of GFP expressing pericytes in green and PDGFRβ cells in the infarct core.The boxes idicates where the pictures of higher magnification were taken, shown in the right panels of single channel PDGFRβ and GFP expressing cells, respectively. The quantification of the number of PDGFRβ and GFP expressing pericytes per mm^2 is presented to the far right. Data is presented as means ± S.D. Statistical analysis was performed using Student's *t*-test, n=6. Scale bars are 20 µm (10 µm for higher magnification images).

Loss of RGS5 Results in Reduced Vascular Leakage and Increased Vascular Density of The Infarct Core

After establishing that loss of RGS5 increases the pericyte coverage of the microvasculature, we moved on to assess if this observation would correlate to increased BBB integrity. For that, we injected Evans blue intravenously 7 days after stroke in RGS5-KO and WT mice to evaluate vascular leakage (Fig. 6A). As expected, we observed that Evans blue permeated the brain parenchyma in the ipsilateral cortical region but not in the unaffected contralateral hemisphere. Interestingly, the vascular leakage was significantly reduced in RGS5-KO compared to WT mice, suggesting that the increased perivascular coverage of pericytes in mice lacking RGS5 expression shows improved barrier integrity (Fig. 6B). Next, we examined whether RGS5 affected the vascular morphology and/or

density within the infarct core. In the contralateral hemisphere, no vascular alterations were observed between genotypes (RGS5-KO and WT). However, in the infarct core, we detected a significant increase in vascular density in the RGS5-KO compared to the WT mice (Fig. 6C).

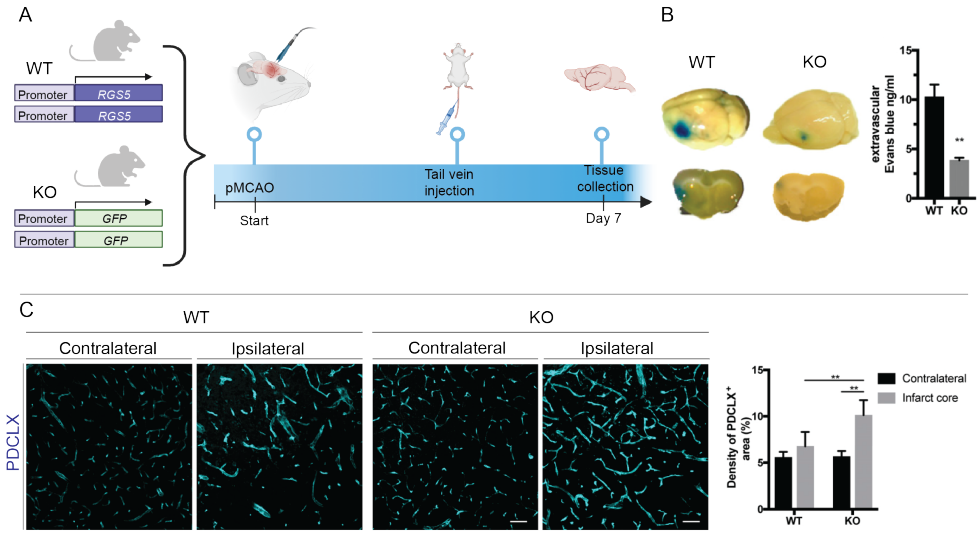

Figure 6. Loss of RGS5 reduces BBB leakage and improves vessel density in the infarct core 7 days after ischemic stroke.

A Schematic of the experimental design where we compared RGS5-KO and WT mice which after the experimental ischemic stroke model pMCAO, received a tail vein injection of Evans blue to assess BBB leakage. **B** Representative images of the whole brain (upper row) and brain sections (lower row) of the different genotypes with Evans blue laekage, 7 days after ischemic stroke. The quantification of extravascular Evans blue is shown to the far right. **C** Representative confocal images of the vasculature within the infarct core positive for PDCLX expression 7 days after ischemic stroke. The left panel shows the WT and the right panel showns the RGS-KO genotype. The quantification of PDCLX$^+$ vessels per designated area is presented to the far right. Data is presented as means ± S.D. Statistics was performed using two-way ANOVA with Tukey's multiple comparisons, n=6. Scale bars are 40 µm.

Paper II | RGS5: A Novel Role as a Hypoxia-responsive Protein That Suppresses Chemokinetic and Chemotactic Migration in Brain Pericytes

As previously established; RGS5 is specifically expressed by mural cells in the brain and loss of RGS5 increases the number of perivascular pericytes upon hypoxic/ischemic injury. However, whether this is due to reduced detachment, increased recruitment or increased survival of pericytes has not been shown. To elucidate the role of RGS5 in hypoxia we silenced RGS5 using siRNA in pericytes and evaluated chemotactic migration in response to PDGFBB, an important growth factor regulating pericyte recruitment and retention at the vasculature.

RGS5 Induction in Hypoxic Pericytes is Regulated on The Protein Level and is Independent of HIF-1α

First, we characterized RGS5 expression in human brain pericytes subjected to hypoxia. Endogenous protein levels of RGS5 remained very low under normal oxygen conditions. In contrast, when pericytes were exposed to hypoxia, RGS5 protein levels were rapidly induced in a time-dependent manner with nearly a 5-fold increase after 1 hour and peaked at 12 hours of hypoxia before they started to decline (Fig 7A, B). The well-known hypoxic transcription factor HIF-1α showed a similar profile with a rapid increase, showing the strongest expression at 6 hours of hypoxia before returning towards baseline (Fig. 7A). However, mRNA levels of RGS5 remained relatively stable throughout the hypoxic time-period and even significantly reduced at 1 hour and 24 hours of hypoxia (Fig. 7C), suggesting that the hypoxic induction of RGS5 happens post-translationally. Nonetheless, RGS5 induction under hypoxia has previously been suggested to be regulated by HIFs (*139*) and to examine that possibility, we directly evaluated if the HIF-1α transcription factor impacts on RGS5 expression using HIF-1α siRNA. Silencing of HIF-1α did not induce a significant change in RGS5 protein levels in any of the assessed time-points of hypoxic exposure, confirming that RGS5 induction is independent of the hypoxia-induced transcriptional network of HIF-1α (Fig. 7D, E).

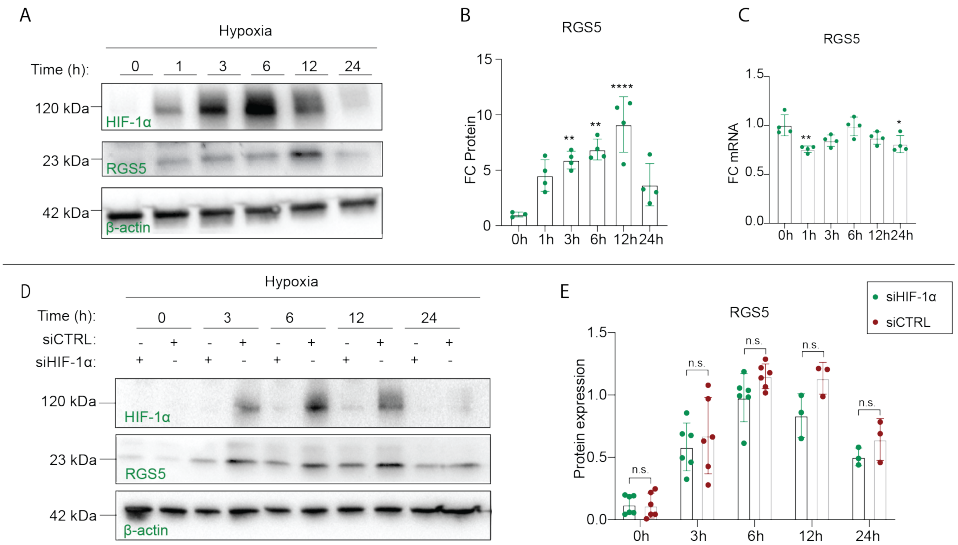

Figure 7. RGS5 is induced under hypoxia, independent of HIF-1α.
A Brain pericytes were exposed to hypoxia (O_2<1%) for 0, 1, 3, 6, 12 or 24 hours. Representative western blot images of RGS5, HIF-1α and (β-actin as housekeeping control). **B** Quantification of relative protein levels of RGS5. **C** Quantification of relative mRNA levels of RGS5. **D** Representative western blot of HIF-1α, RGS5 and β-actin after pericytes were exposed to hypoxia for 0, 3, 6, 12 or 24 hours. **E** Quantification of RGS5 protein expression in pericytes treated with HIF-1α siRNA or scrambled control siRNA and exposed to hypoxia for 0, 3, 6, 12 or 24 hours. Data is presented as means ± S.D. Statistical testing was performed using one-way ANOVA with Tukey's multiple comparison (B, C) or multiple *t*-tests (E), n=3 – 6. Significance was set at $p \leq 0.05$.

RGS5 Desensitizes Pericytes to PDGFBB-induced Chemotaxis

Pericytes recruitment and retention to the endothelium is actively modulated by the release of chemotactic factors such as PDGFBB that attract pericytes to the vascular wall. To assess the role of RGS5 in hypoxia we silenced RGS5 with siRNA (siRGS5) and compared that to a scrambled control siRNA (siCTRL). Next, we used a microfluidic chamber that produces a stable linear concentration gradient of PDGFBB and measured pericyte chemotactic migration (Fig. 8A). Silencing RGS5 in hypoxic pericytes resulted in a significantly increased sensitivity to PDGFBB, where pericytes migrated parallel towards the concentration gradient. In contrast, RGS5 expressing pericytes in the siCTRL condition exhibited a more random migration and did not display a clear chemotactic phenotype (Fig. 8B). Quantification of cellular trajectories revealed that the forward migration index (FMI) parallel to the gradient was significantly higher in RGS5 silenced pericytes compared to the control (Fig. 7C).

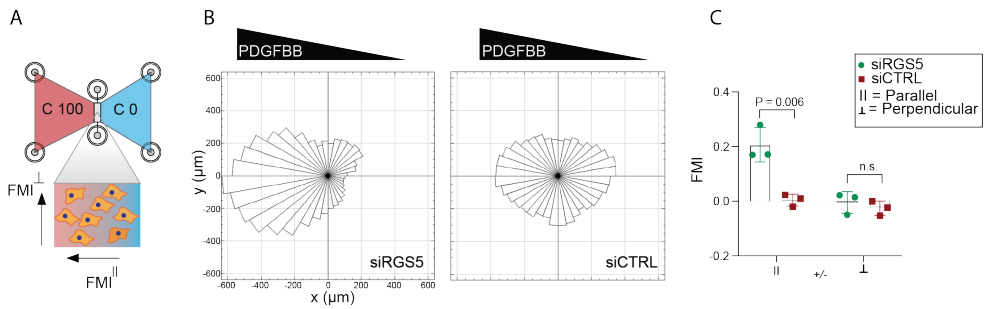

Figure 8. RGS5 desesitizes pericytes to PDGFBB chemotactic cues under hypoxia.
A Illustration of microfluidic chemotaxis µ-slides used for chemotactic evaluation that produces a stable linear concentration gradient from concentration (C) 100% to 0%. Chemotactic migration evaluation was based around FMI$^{\parallel}$ parallel to the gradient or FMI$^{\perp}$ perpendicular to the gradient. **B** The role of RGS5 on chemotactic migration in response to a PDGFBB concentration gradient with C 100% being (50 ng/ml) and tracked using live-imaging for 22 hours of hypoxia. The sum of 160 cellular trajectories from siRGS5 or siCTRL pericytes are displayed in rose plots. **C** Quantification of the parallel and perpendicular FMI. Data is presented as means ± S.D. Statistical testing was performed using multiple *t*-tests, n=3.

Paper III | Pericyte-specific Secretome Profiling Using TurboID in an *In Vitro* Blood-Brain Barrier Model

Cell-cell communication is paramount to maintain homeostasis in the brain under physiological conditions but is also important to instigate a response to pathological stimuli such as hypoxia or ischemia. Pericytes have been shown to have an extensive secretome, but the current knowledge is mostly limited to *in vitro* monocultures and a full characterization of the pericytes secretome profile in hypoxia has been lacking. To examine the hypoxic pericyte-secretome profile in more complex multi-

cellular environments, we used the biotin ligase TurboID to label secreted factors of pericyte origin, in co-culture with human endothelial cells and human astrocytes.

TurboID Biotinylates Pericyte-Secreted Proteins in Spheroid Co-Cultures

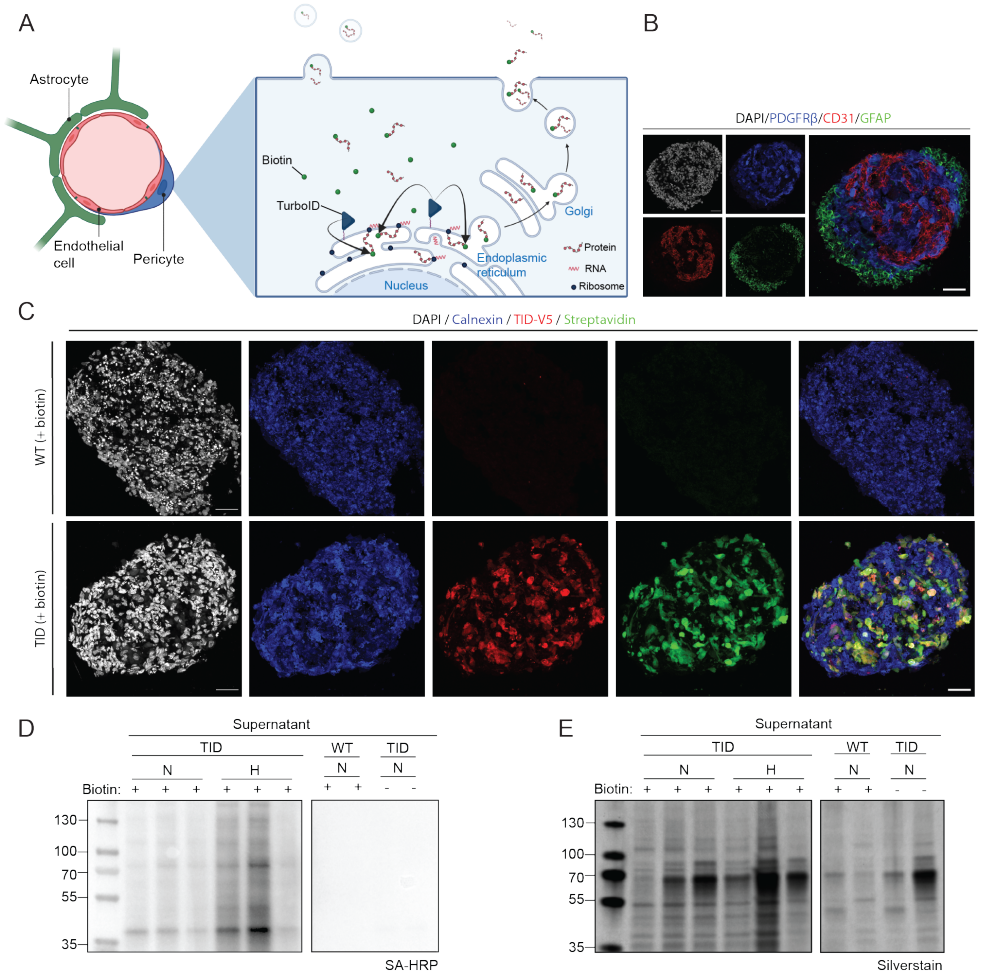

Figure 9. TurboID biotnylates intracellular and secreted proteins of pericyte origin in spheroid co-cultures. **A** Illustration of co-culture cell types. The zoomed in picture showsTurboID anchored to endoplasmic reticulum (ER) in pericytes which labels proximal proteins in the range of ~20 nm and the conventional secretory pathways via ER/Golgi trafficking or release of extracellular vesicles. **B** Section of a spheroid stained for PDGFRβ (pericytes, blue), CD31 (endothelial cells, red) and GFAP (astrocytes, green). **C** Spheroids with either TurboID-expressing pericytes or WT-pericytes, treated with 500 µM of exogenous biotin and stained for the ER-marker calnexin (blue), V5-tagged TurboID (red), streptavidin for biotin labelling (green) and DAPI (white). **D** Streptavidin blotting of supernatant samples from spheroids harvested 24 hours after biotin treatment. **E** Total protein content of the same samples were analysed by silverstain. Abbreviations: N, Normoxia; H, Hypoxia; TID, TurboID. Scale bars are 50 µm.

TurboID has been extensively used as biotin ligase to study protein-protein interactions, but few studies have utilized TurboID to label the secretome of specific cell types (*183*). Since most proteins translated in the endoplasmic reticulum (ER) are destined for secretion, we generated a stable cell line of pericytes expressing an ER-anchored TurboID protein facilitating biotin labelling of secreted molecules (Fig. 9A). To validate if pericyte-specific labelling was possible in co-culture conditions, we generated spheroids of human TurboID-expressing pericytes, endothelial cells and astrocytes. PDGFRβ^{+} pericytes and CD31^{+} endothelial cells were distributed evenly throughout the spheroid while GFAP^{+} astrocytes occupied the spheroid border (Fig 9B). Next, we evaluated TurboID activity by measuring biotin-labelling of endogenous proteins using immunocytochemistry. Endogenous proteins were clearly biotinylated, evident from the streptavidin immunostainings in the TurboID-expressing pericytes compared to WT-pericytes having no, or very low, streptavidin signal. Furthermore, streptavidin labelling co-localized to the TurboID V5-tag and the endoplasmic reticulum marker calnexin (Fig. 9C). As immunocytochemistry evaluation cannot distinguish between intracellular and extracellular proteins, we evaluated the cell culture supernatant for the presence of secreted biotinylated proteins using western blotting. We detected a clear signal from streptavidin-blotting in both normoxic and hypoxic conditions in TurboID-pericytes in the presence of exogenous biotin, indicating successful biotinylation. Importantly, our negative controls WT-pericytes or TurboID-pericytes with omitted exogenous biotin had undetectable levels of biotinylated proteins whilst a strong signal from the total protein content was observed in the silver stain (Fig. 9D, E).

Proteomics of The Pericyte Secretome in Hypoxia

To characterize the pericyte secretome in hypoxia we performed shotgun proteomics. Furthermore, we analysed the differences in protein identities between monocultures of pericytes compared to pericytes cultured in spheroids. For that, we purified biotinylated proteins from the cell cultures supernatants using streptavidin-biotin affinity pull-downs and samples were analysed using LC-MS/MS (Fig. 10A). From the purified supernatant samples, we detected on average over 2,000 different proteins, suggesting that a large fraction of the pericyte secretome was biotin labelled. An UpSet plot of our mass spectrometry dataset indicated differentially expressed proteins between experimental conditions. For instance, we identified 33 and 20 proteins that were significantly different and specific in hypoxic compared to normoxic pericytes in monocultures or spheroid cultures, respectively. Interestingly, we observed the largest differences in secreted proteins between monocultures and spheroid cultures, regardless of experimental condition (hypoxia or normoxia). Specifically, we identified 73 secreted proteins that were significantly different between hypoxic spheroids (HS) and hypoxic monocultures (HM). Furthermore, 87 proteins were significantly different and specific when comparing normoxic spheroids (NS) to normoxic monocultures (NM), demonstrating that the

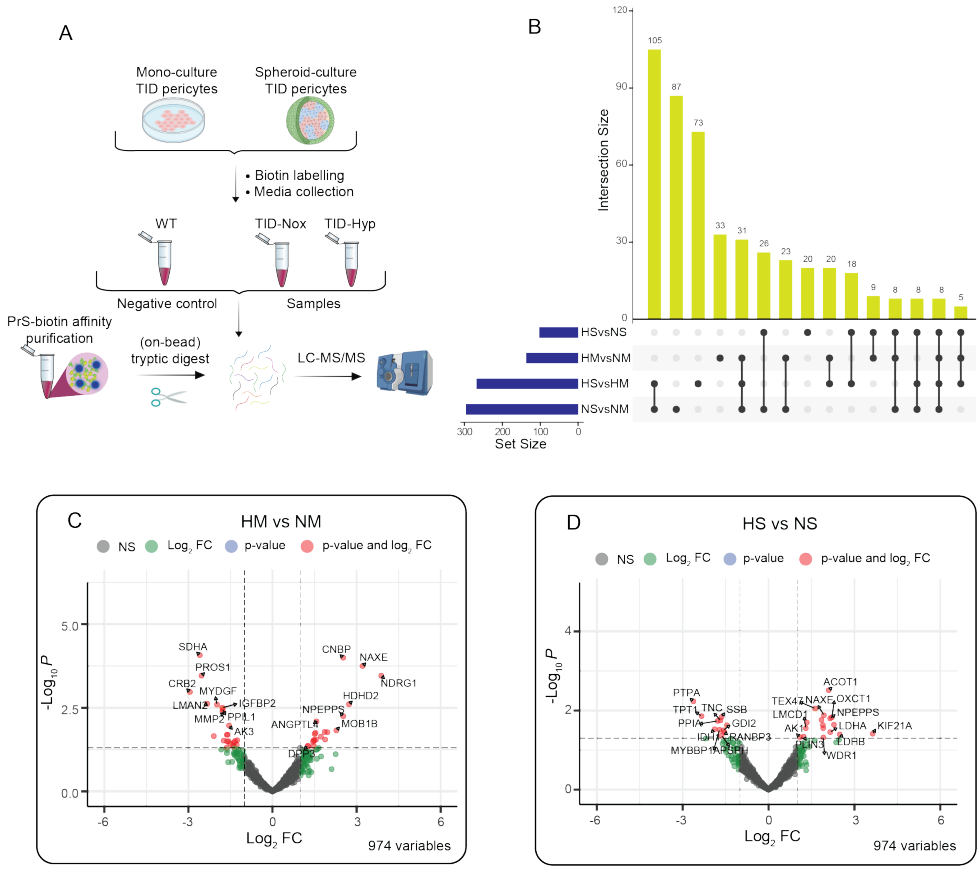

Figure 10. Proteomics of the pericyte-specific secretome profile in hypoxia.
A Experimental design wehre cell culture supernatant was extracted from pericyte monocultures and spheroid cultures after 24 hours of normoxia or hypoxia with WT as negative control. Supernatants containing biotylated proteins of pericyte origin were purified using protease resistant strepatvidin beads (PrS)-biotin affinity pull-downs where proteins underwent trypic digestion before peptides were anlysed by LC-MS/MS. B UpSet plot showing shared or specific – differentially expressed proteins between the experimental conditions. C Volcano plot showing the differentiall expressed proteins between HM versus NM. D Volcano plot showing the differentially expressed proteins between HS versus NS. Abbreviations: TID, TurboID; HM, Hypoxia monoculture; NM, Normoxia monoculture; HS, Hypoxia spheroids; NS, Normoxia spheroids.

cell-cell interactions at the BBB have a large impact on the pericyte secretome (Fig. 10B). To give additional insight into the secretome profile of pericytes we generated volcano plots showing the significant differences in the binary comparisons between hypoxia and normoxia. In monocultures (HM vs NM), some of the top hypoxia-enriched secreted proteins included cellular nucleic acid binding protein (CNBP), NAD(P)HX epimerase (NAXE), N-Myc downstream regulated gene 1 (NDRG1), angiopoietin-like 4 (ANGPTL4) and others. In contrast, we observed a significant downregulation of succinate dehydrogenase complex subunit A (SDHA), protein S (PROS1), insulin-like growth factor binding protein 2 (IGFBP2), and matrix

metalloproteinase-2 (MMP2) (Fig. 10C). Interestingly, the spheroid culture comparison (HS vs NS) displayed a different pericyte secretome profile. Here, some of the most significant hypoxia-enriched secreted proteins of pericyte origin included Acyl-CoA thioesterase 1 (ACOT1), NAXE, 3-oxoacid CoA-transferase 1 (OXCT1), alanine aminopeptidase (NPEPPS), while we observed a downregulation of proteins such as protein phosphatase 2A (PTP2A), tumour protein-translationally-controlled 1 (TPT1), and others (Fig. 10D). Notably, although some of the differentially expressed proteins in hypoxic compared to normoxic pericytes were conserved between monocultures and spheroid cultures such as NPEPPS and NAXE, a majority of differentially expressed proteins were unique to its respective cell culture condition. Together, these results support that pericytes display a different secretome profile in response to hypoxia and that their secretory response is highly dependent on cell-cell interactions between BBB-residing cells.

Paper IV │Pericyte-derived Microvesicles as Plasma Biomarkers Reflecting Brain Microvascular Signalling at Different Stages of Acute Ischemic Stroke

Identification of circulating biomarkers that can be detected in peripheral blood is still an unmet need in stroke research. The cellular release of MVs has great potential to not only serve as a biomarker but also potentially reflect the pathogenesis of stroke evolution. While pericytes are known to release MVs, previous studies are mostly limited to *in vitro* or animal models and whether the characteristics of pericyte-derived MVs from blood plasma changes after ischemic stroke is not known. To assess whether pericyte-derived MVs can serve as a plasma biomarker we analysed blood samples from patients at different timepoints after stroke onset compared to controls (Fig. 11A).

Ischemic Stroke Leads to an Early Increase in Pericyte-Derived MVs

The plasma levels of pericyte-derived MVs in the hyperacute phase 0-6 hours after ischemic stroke onset, did not show a significant difference compared to the control group. However already at 12-24 hours after ischemic stroke, the concentration of pericyte-derived MVs was significantly higher in stroke patients compared to controls (median [range], 1569 [108-4755] MVs/µl versus 658 [18-2971] MVs/µl; $P < 0.0002$. Furthermore, the increase in circulating pericyte-derived MVs was sustained up to 2-6 days in stroke patients compared to controls (1300 [26-5187] MVs/µl versus 658 [18-2971] MVs/µl; $P = 0.0076$ (Fig. 11B).

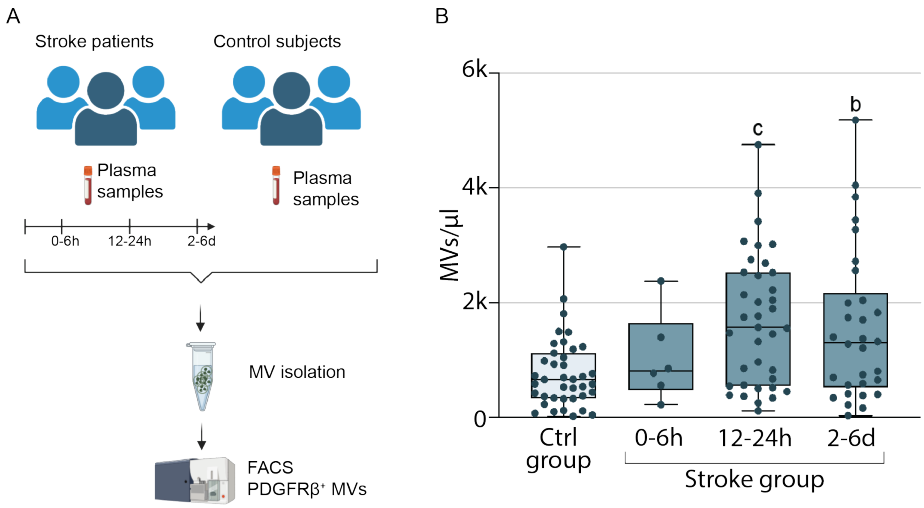

Figure 11. Early increase of circulating pericyte-derived MVs after ischemic stroke onset.
A Overview of experimental design. **B** Box plots showing the quantification of pericyte-derived MVs analysed from blood plasma in stroke patients between 0-6 hours, 12-24 hours or 2-6 days after stroke onset compared to the control group. Statistical testing was performed using Mann-Whitney nonparametric test. $P^b < .01$, $P^c < .001$.

The Protein Cargo of Pericyte-Derived MVs Displays Temporal Changes After Ischemic Stroke Onset

Next, we evaluated the protein cargo of the isolated pericyte-derived MVs at the different time points after ischemic stroke onset compared to controls. At the hyper-acute phase (0-6 hours) after stroke onset, the protein level of pericyte-derived MVs in stroke patients was significantly decreased compared to controls. Many of the downregulated proteins corresponded to inflammatory chemokines or cytokines such as cluster of differentiation 40 (CD40), interleukin (IL)-17C, IL5, IL6 and IL2 (Fig 12A).

Interestingly, between 12-24 hours after stroke onset, the protein cargo of pericyte-derived MVs in stroke patients displayed an upregulation in proangiogenic and proinflammatory signalling molecules, possibly reflecting the pathogenesis of ischemic stroke. Some of the most significantly upregulated proteins included matrix metalloproteinase-1 (MMP-1), CD244, MCP-4, CXC-motif chemokine 5 (CXCL5) and vascular endothelial growth factor A (VEGF-A) (Fig 12B). Between 2-6 days after ischemic stroke onset, pericyte-derived MVs in stroke patients maintained significantly increased protein levels of proangiogenic and proinflammatory molecules such as MMP-1, VEGFA, CD40, and CXCL5 compared to the control group (Fig. 12C).

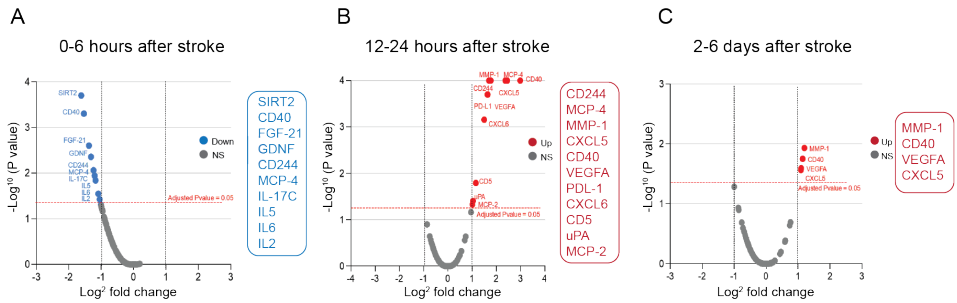

Figure 12. The protein cargo of pericyte-derived MVs in stroke patients compared to controls.
A Volcano plots showing the differentially expressed proteins in pericyte-derived MVs betwwen ischemic stroke patients compared to controls between 0-6 hours, **B** between 12-24 hours, and **C** between 2-6 days. Statistical testing was performed using two-way ANOVA with Tukey's multiple comparison.

Paper V | The Transcriptional Landscape of Pericytes in Acute Ischemic Stroke

Stroke pathology is a complex process involving different responses of various types of brain cells. The specific roles of distinct cell subpopulations after stroke further contribute to its complexity. Transcriptome studies have the potential to characterize cellular heterogeneity and provide a deeper understanding of the molecular mechanisms involved in stroke pathology. Since ischemic stroke develops rapidly and has a narrow time window of treatment, a better understanding of the pathological progression during the acute phase may be crucial for early and effective interventions. As such, we aimed at elucidating the transcriptome changes using 10x genomics at different time points of the acute phase of ischemic stroke using a mouse pMCAO model, where our main aim was to characterize the pericyte response and differences between subpopulations of pericytes within the vascular niche.

Transcriptional Analysis and Identification of Different Cell Populations in The Acute Phase

For transcriptome analysis, brain cells depleted from mature neurons were isolated from either the ipsilateral (ipsi) or contralateral (contra) stroke region at 1, 12, or 24 hours after MCAO. Since the cells were isolated by enzymatic digestion and from different conditions (ipsi vs contra), that could result in differential expression of certain surface markers of specific cell populations, we isolated all live cells to ensure an unbiased approach (Fig. 13A). All single cells were projected on UMAP

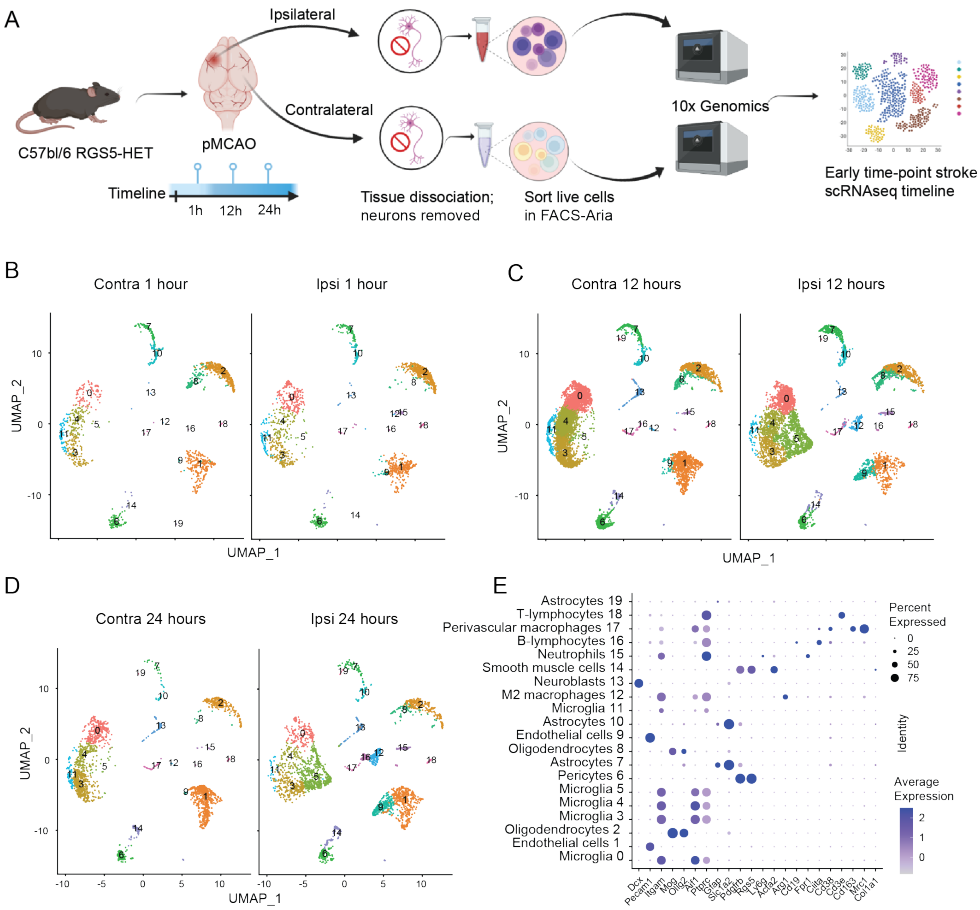

Figure 13. Single cell RNA-sequencing of neuron-depleted live brain cells at 1, 12, and 24 hours after pMCAO. **A** Schematics of the experimantal design and workflow. **B-D** UMAP plots of the identified clusters in the contra or ipsi condition at different time points of the acute phase after ischemic stroke. **E** Cell types identified by clustering analysis and genes defining cell type identity.

plots after batch-effect correction showing clear separation between different cell populations at the 3 different time points (Fig. 13B-D). Detection of known cell type markers or combination of genes unambiguous for specific cell types identified 19 different clusters including microglia (*ITGAM*$^{+}$, *AIF1*$^{+,}$ *PTPRC*$^{+}$), astrocytes, (*GFAP*$^{+,}$ *SLCLA2*$^{+}$), oligodendrocytes (*MOG*$^{+}$, *OLIG2*$^{+}$), endothelial cells (*PECAM1*$^{+)}$, smooth muscle cells (*PDGFRβ*$^{+}$, *RGS5*$^{+}$, *ACTA2*$^{+}$), pericytes (*PDGFRβ*$^{+}$, *RGS5*$^{+}$, *ACTA2*$^{-}$), as well as others (Fig. 13E). Notably, we observed large changes in cellular clustering at 12 and 24 hours between the ipsilateral and contralateral hemispheres. For instance, endothelial cluster 9, microglial cluster 5 and immune cells like macrophages, B-cells, T-cells, and neutrophils showed an increased density in the ipsilateral stroke region (Fig. 13B-D).

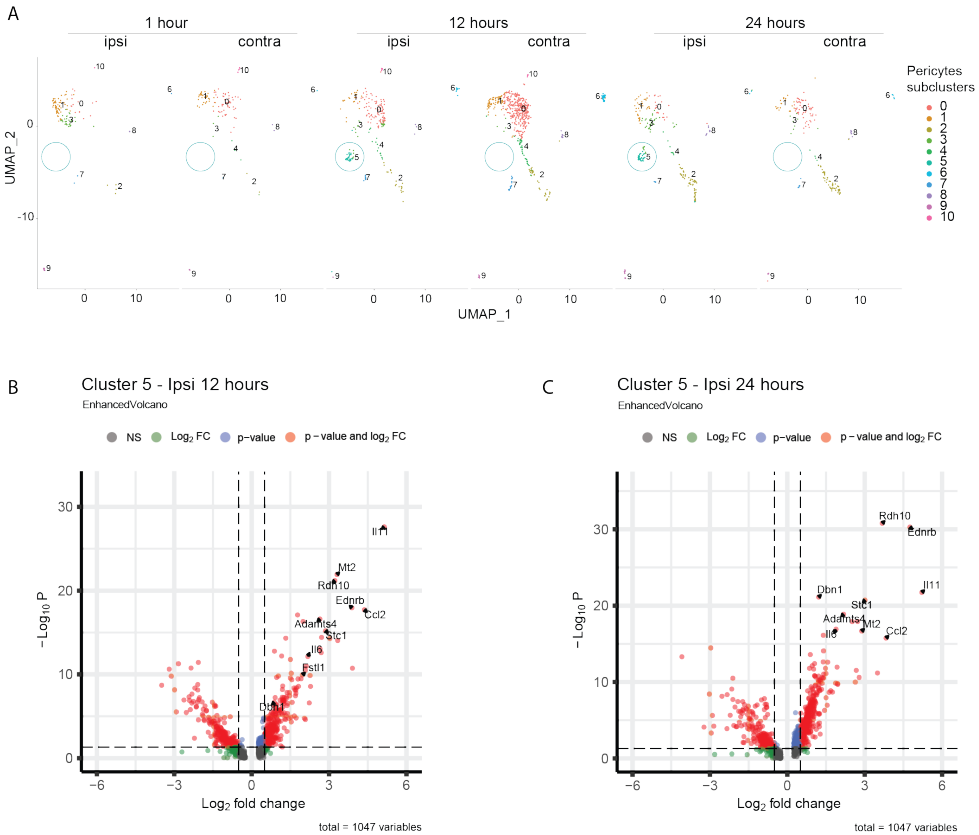

Figure 14. Heterogenous subpopulations of pericytes in the acute phase of stroke.
A The re-clustering of the pericyte population revelaled 8-10 different pericyte subclusters depending on the time point and ipsi versus contra hemispheres. The stroke specific subluster 5 appearing at 12 and 24 hours after stroke is indicated by the green circle. **B-C** Volcano plot showing the genes that are differentially regulated in the ipsi cluster 5 compared to the remaining pericyte clusters at 12 hours and at 24 hours after ischemic stroke.

Exploring the Dynamic Heterogeneity of Pericyte Subpopulations During the Acute Phase of Ischemic Stroke

To delve deeper into the pericyte transcriptomic response after ischemic stroke, we isolated pericytes and smooth muscle cells from the dataset and performed a new clustering analysis. Due to pericytes plasticity, this approach aimed to get a more comprehensive understanding of the possible subtypes of perivascular cells. The re-clustering revealed 8-10 different subclusters depending on time point and experimental condition (ipsi vs contra). Interestingly, at 12 and 24 hours after stroke we detected the pericyte subcluster 5 (*RGS5*$^{+}$, *PDGFRβ*$^{+}$, *ACTA2*$^{-}$), specific to the ipsilateral stroke region, suggesting a unique stroke-specific pericyte subpopulation (Fig. 14A). To better characterize the stroke-specific cluster 5 of pericytes, we

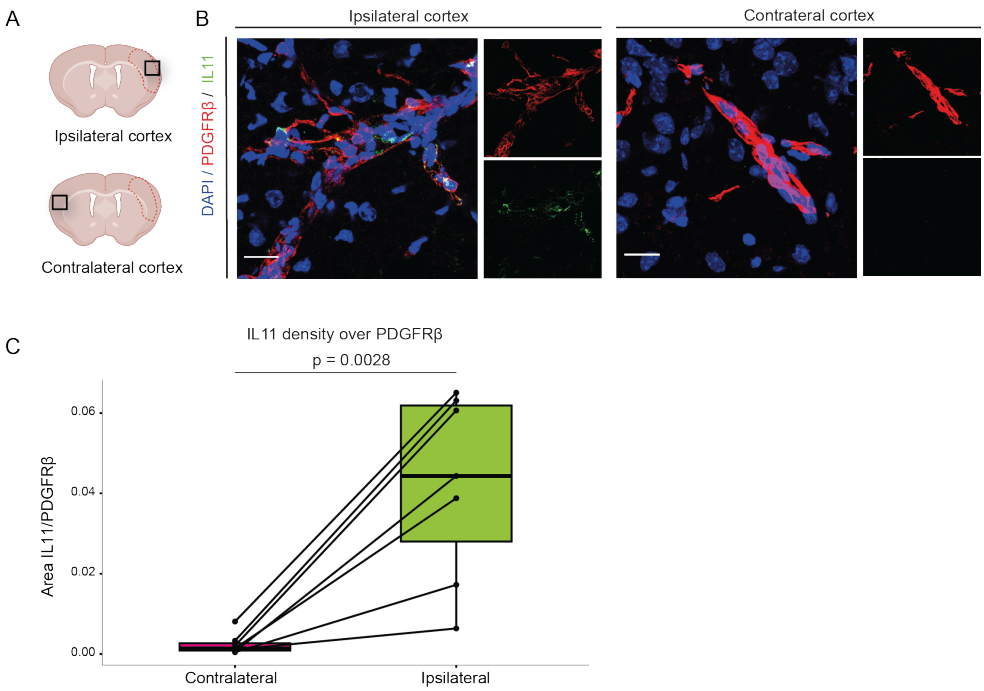

Figure 15. IL11 protein expression is restricted to PDGFRβ cells in the stroke region.
A Location of the selected images in black boxes, where the infarct core is outlined in red. **B** Confocal images showing PDGFRβ and IL11 expressing cells. **C** Area fraction occupied by PDGFRβ and IL11 expressing cells. Statistical testing was performed using paired Students *t*-test, n=7. Scale bar 20 µm.

investigated the differentially expressed genes (DEGs) of cluster 5 to the remaining pericyte clusters. Although we observed the largest fold change in different gene expressions at 24 hours after stroke, the majority of the DEGs present in subcluster 5 were conserved and significantly different both at 12 and 24 hours after stroke. The top 10 most upregulated genes after stroke in cluster 5 included IL11, IL6, retinol dehydrogenase (RDH10), endothelin receptor B (EDNRB), C-C motif chemokine ligand 2 (CCL2), metallothionein-2 (MT2), stanniocalcin 1 (STC1), ADAM metallopeptidase (ADAMTS4), drebrin 1 (DBN1), and follistatin like 1 (FSTN1) Fig. 14B, C).

From the bioinformatic analysis of our sequencing data, we found IL11 to be among the highest upregulated genes and specific to the pericyte subcluster 5. IL11 is a cytokine known to be primarily produced by stromal fibroblasts within different organs but has not previously been associated with pericytes (*184, 185*). To further identify if the altered gene expression of IL11 could be detected on the protein level, we also conducted immunofluorescence evaluation to evaluate IL11 expression in stroke-responsive pericytes. Indeed, we confirmed the specific ischemic-injury

related upregulation of IL11 was confined to PDGFRβ-expressing cells and the increase was significant compared to the contralateral hemisphere (Fig. 15A-C).

Discussion and Future Perspectives

In the work presented in this thesis, the overarching aim was to elucidate the role of the pericyte response to pathological hypoxia and ischemic stroke. The first two studies focused on the role of RGS5, a marker of activated pericytes and a possible candidate to modulate pericytes response to hypoxia/ischemia. The rationale behind RGS5 being one of our proteins of interest had several reasons: one was that RGS5 expression is specific to mural cells in the brain; another was the dynamic nature of RGS5 expression in various physiological or pathological conditions, indicating a role in adaptive responses. For instance, RGS5 expression shows large fluctuations in the developing foetal vasculature in mice, with the highest expression around E14.5, before it declines and remains low in adult animals under physiological conditions (*136, 137*). These observations support the hypothesis that a dynamic regulation of RGS5 expression may be important during vasculogenesis while the mature and quiescent vasculature in the adult is associated with pericytes exhibiting low RGS5 levels. Notably, in adult mice, RGS5 expression is altered in response to certain environmental cues and an upregulation has been consistently observed in hypoxic or ischemic pathologies, associated with vessel abnormalities and pericyte detachment from the vascular wall (*133, 138, 181*).

In paper I, we showed that loss of RGS5 results in increased numbers of perivascular pericytes while the density of parenchymal PDGFRβ$^+$ cells was reduced, 7 days after stroke. These observations suggest RGS5 to be a regulator of important adaptive processes in the chronic phase of stroke such as vascular remodelling and scar formation. The increased perivascular density of pericytes in RGS5-KO mice is important for vascular maturity and integrity within the infarct core, which correlated with reduced vascular leakage. At the same time, the reduction of PDGFRβ$^+$ cells in the parenchyma of RGS5-KO animals could affect the fibrotic scar formation, as previous studies support that a subpopulation of parenchymal PDGFRβ-expressing pericytes can contribute to fibrosis (*148, 149*). This shift in spatial distribution of pericytes in RGS5-KO mice could have several reasons. The reduction of PDGRβ$^+$ cells in the parenchyma may be due to reduced detachment of pericytes but it is also possible that the increased microvascular integrity observed in RGS-KO mice, reduces the invasion of immune and fibrotic cells into the infarct core, resulting in reduced numbers of e.g., scar forming fibroblasts. The increase of perivascular pericytes may be due to reduced pericyte detachment from the vascular wall, increased cell proliferation, improved survival, or increased migration of

pericytes to the newly formed vessels. To elucidate the role of RGS5 as a regulator of pericytes response after ischemic stroke, we cultured human brain pericytes to study if RGS5 regulates these cellular processes *in vitro*.

In paper II, we established RGS5 as an oxygen-sensing protein that is rapidly stabilized under hypoxia, while very low to non-detectable levels of RGS5 were observed in normoxic conditions, in brain pericytes. In contrast to previous observations (*139*), we did not find a link between RGS5 expression and HIF-1α activation, but instead, the rapid induction of RGS5 under hypoxia happens post-translationally likely due to inhibition of the oxygen dependent proteolytic N-degron pathway (*142*). One of our hypotheses behind the increased numbers of perivascular PDGFRβ^{+} pericytes in RGS5-KO mice observed in the infarct core in paper I, was that RGS5 affects the migration of pericytes. A key component in pericytes association to the microvasculature is the active regulation of chemotactic signals released by endothelial cells such as PDGFBB, which regulates the recruitment and retention of PDGFRβ^{+} pericytes to the vascular endothelium. We showed that RGS5 stabilization in hypoxia desensitizes pericytes to PDGFBB induced chemotaxis, which could be a contributing factor in regulating the association of pericytes to vascular endothelial cells. In addition, we show that RGS5 does not affect pericyte proliferation or survival under hypoxia (*Fig.5 in paper II*), suggesting that the increase in perivascular pericytes in RGS5-KO mice after stroke, could be the result of an altered migratory phenotype. However, such claims would require mechanistic verification *in vivo*, in support of the RGS5/PDGFRβ-regulation of perivascular coverage and pericyte migration. Notably, numerous other mechanisms affecting pericyte coverage may be regulated by RGS5. Previous studies support RGS5 having a regulatory role in WNT, TGF-β and hedgehog signalling, all of which are important in angiogenesis and vascular remodelling that could regulate pericyte rarefaction at the vascular wall (*186-188*). Future studies, looking at transcriptome changes in RGS5 deficient mice after stroke or phospho-proteomic analysis of hypoxic pericytes lacking RGS5 would provide a more comprehensive understanding of specific cellular mechanisms where RGS5 may be involved. Still, RGS5's prominence in the vascular niche remains evident, making it a prime candidate for therapeutic intervention.

An interesting observation from these studies is that the stabilization of RGS5 in hypoxia would appear to be an adaptive response to compromised tissue oxygenation, yet paradoxically, loss of RGS5 seems to promote essential mechanisms of pericyte recruitment and improve stroke outcome in mice. It is conceivable that the ability of RGS5 to be dynamically regulated in response to oxygen fluctuations is an important mechanism to fine-tune highly regulated oxygen-sensitive processes like angiogenesis, requiring temporal control of detachment and subsequent recruitment of pericytes under physiological conditions (e.g., during development). However, in vascular pathology such as ischemic stroke, tissue oxygenation is dramatically reduced, and the severe hypoxia likely leads to

the rapid and prolonged stabilization of RGS5. Under such pathological conditions, conserved evolutionary mechanisms of oxygen-sensing such as regulation of RGS5 via the N-degron pathway, may be an example of when adaptation to hypoxia becomes excessive, and transforms into maladaptation.

The following two studies were centred around characterizing the pericyte secretome in hypoxia and ischemic stroke. Studying cellular secretomes has long relied on the use of *in vitro* monoculture models allowing controlled conditions with certain association between secreted molecules and their cellular origin. Albeit useful for specific purposes, these systems are poorly resembling *in vivo* conditions, confounding the interpretation of existing data. In paper III, I present a method for pericyte-specific secretome profiling in an *in vitro* co-culture model of the BBB, by using the biotin ligase TurboID that enables biotin-tagging of pericyte-secreted proteins that can later be purified and analysed. This approach allowed us to not only characterize the secretome profile of pericytes in response to hypoxia but to compare the differences in pericyte-secreted factors between monocultures and co-cultures. While previous studies have underscored that maintaining BBB homeostasis is dependent on the crosstalk between its constituent cells (*189, 190*), the influence of cell-cell interactions on the pericyte secretome has not been previously described. The mass spectrometry analysis revealed a variety of well-characterized secreted proteins that were differentially regulated between normoxic and hypoxic pericytes. While we observed that some of the differentially secreted proteins between normoxic and hypoxic pericytes were conserved in both mono- and co-cultures e.g., NAXE and NPEPPS, most differentially secreted factors were unique to their respective culture conditions. These observations highlight the importance of cell-cell signalling networks between BBB-residing cells and can possibly provide more accurate data of the pericyte secretome profile in hypoxia. However, even though this model provides a more sophisticated cell culture approach of studying the secretome of brain pericytes, organs like the brain are far too complex to fully recapitulate *in vitro* or even *ex vivo*. Future studies, incorporating TurboID biolabeling in animals would provide an even better representation of the pericyte secretome while at the same time reflecting the possible signalling perturbations that occur in complex pathologies such as ischemic stroke.

Besides relying on labelling of cell type secretomes there are also other ways to study cell-specific secreted factors. In paper IV, we studied pericyte-derived MVs present in the blood plasma of ischemic stroke patients at different time points of the acute phase. Since MVs originate from the plasma membrane they carry surface antigens (such as PDGFRβ), allowing them to be traced back to their cellular origin. These MVs function as vehicles carrying bioactive cargo from the parental cell that can affect the biochemical state of recipient target cells. The level of MVs found in plasma are known to change in various diseases and the MV-cargo reflects the state of the parental cell (*191, 192*). As such, MVs are promising targets to serve both as

biomarkers of stroke but could also reflect important signalling processes during pathogenesis.

At the start of this project, several other studies had explored the possibility of using MVs as biomarkers of stroke where most studies were focused on endothelial cells (*165*). Yet, to our knowledge, no previous study had examined the potential use of pericyte-derived MVs, reflecting the vascular signalling in acute ischemic stroke. Because of pericytes unique location at the blood/brain interface and their early response to ischemic injury, pericytes could constitute a novel source of peripheral biomarkers, which is still an unmet need in acute stroke care. Confirming our *a priori* hypothesis, that pericytes mount an early response to ischemia, we detected significantly higher plasma levels of pericyte-derived MVs already at 12-24 hours which persisted up to 2-6 days in human stroke patients. These observations support the potential use of pericyte-derived MVs as an easy and practical method that could complement existing diagnostic tools and reflect the temporal evolution of ischemic stroke. However, an important factor to consider is that for a biomarker to be useful, it needs to be specific for its designated pathology. As stroke mimics accounts for almost half of hospital admissions (*193*), future studies will have to determine the reliability of pericyte-derived MVs for accurate stroke diagnosis.

Besides the role as a possible biomarker, MVs cargo may reflect important signalling mechanisms that modulates the pathological progression after stroke. When analysing the cargo of pericyte-derived MVs, we noticed a temporal switch, indicating an anti-inflammatory profile at 0-6 hours, whereas the later timepoints of the acute phase was associated with an increase of proinflammatory and proangiogenic molecules. These findings may suggest a beneficial role of the pericyte secretome after ischemic stroke, possibly limiting the acute inflammatory response while initiating recovery mechanisms such as angiogenesis and vascular maturation at later time points after stroke onset. However, it is important to remember that the MV cargo only reflects a small portion of the cellular secretome and analysing peripheral samples does not take into consideration the paracrine signalling of other soluble factors that are released by ischemia challenged pericytes.

In our final approach of investigating pericyte's response to ischemic stroke, we used single cell RNA-sequencing that provided us with a large-scale dataset to analyse transcriptome changes in brain pericytes. In the light of known pericyte heterogeneity in morphology and marker expression we identified several unique transcripts that changed over time in the acute phase of ischemic stroke. Specifically, we identified a subset of pericytes that were stroke-specific at 12 and 24 hours after stroke onset, which were characterized by an upregulation of a specific set of genes such as *IL6, IL11, CCL2, EDNRB, ADAMTS4, STC1* and *RDH10*. Interestingly, these results were confirmed in a recent study showing an upregulation of most of the genes present in the stroke-specific pericytes after using a transient model of ischemic stroke in mice (*172*). This differential transcriptional program could either represent different pathological states of pericytes in stroke or

indicate the existence of different pericytes subpopulations. Since our method of single cell RNA-sequencing does not consider spatial resolution, it is possible that the pericyte heterogeneity is due to their location within the stroke affected brain region, affecting their response.

Nonetheless, our results indicated that the activated states of the stroke-specific cluster were associated with the upregulation of numerous immune regulatory genes including IL6, IL11, and CCL2. Moreover, we found IL11 to be one of the most significantly upregulated genes which was also unique to the stroke-specific pericytes. As transcriptome changes do not always translate to differences in protein levels, we confirmed our findings by immunostainings showing a significant difference in IL11 expression within the infarct core compared to the control which was restricted to PDGFRβ-positive cells. Previous studies have suggested a biphasic role of IL11 in terms of homeostasis, fibrosis and inflammation in ischemic stroke (*194*). As such, future studies are needed to determine its role in the acute phase of stroke. Furthermore, our correlational observations of pericyte transcriptional levels in response to stroke provides valuable insights on potential therapeutic targets but it remains difficult to determine a causal relationship between specific genes and the pathology. Functional knock-out studies on potential stroke-specific targets such as IL11 would provide valuable insights in determining the role of specific genes and whether their activation improves or exacerbates stroke outcome.

One of the strengths from this study is our temporal evaluation of the pericyte transcriptome in the acute phase of stroke, shedding further light on pericyte heterogeneity and functional responses during stroke evolution. As ischemic stroke pathology progresses for weeks, it would be important for future studies to also characterize the temporal transcriptional landscape at more advanced stages of the disease to pave the way for identification of novel therapeutic targets.

In conclusion, this thesis aimed at expanding the current understanding of the response of pericytes to ischemic stroke. Towards that goal we have studied that from several different angles and in various contexts from human stroke patients to animal or cell culture models that recapitulate stroke conditions. Our presumptions of RGS5 being an important regulator of pericytes response to ischemic injury based on existing literature was confirmed and we identified RGS5 as possible target that could modulate neurovascular protection after ischemic stroke. However, specific mechanisms behind the effect of RGS5 in ischemic stroke remains to be clarified. Understanding the complex pathological cascade in ischemic stroke is no easy task and involves specific responses of various brain cell types affected by the ischemic injury. To increase our knowledge of stroke pathology, it is important to understand specific cellular responses, without compromising the physiological relevance of the multicellular interaction within the brain. In that regard, most of the papers in this thesis has aimed at examining pericyte-specific responses while maintaining a more or less physiologically relevant experimental model and our results also strengthen the importance of cell-cell interactions in regulating the pericyte

secretome. Overall, our results highlight the diverse and dynamic nature of pericytes exhibiting rapid transcriptome, secretome and specific protein regulation after hypoxic insult, suggesting that targeting pericytes could be of clinical relevance in ischemic stroke.

References

1. A. H. Knoll, M. A. Nowak, The timetable of evolution. *Science Advances* **3**, (2017).
2. D. B. Cole *et al.*, On the co-evolution of surface oxygen levels and animals. *Geobiology* **18**, 260-281 (2020).
3. A. J. Krause *et al.*, Stepwise oxygenation of the Paleozoic atmosphere. *Nature Communications* **9**, (2018).
4. J. R. Nursall, Oxygen as a Prerequisite to the Origin of the Metazoa. *Nature* **183**, 1170-1172 (1959).
5. E. U. Hammarlund, Harnessing hypoxia as an evolutionary driver of complex multicellularity. *Interface Focus* **10**, (2020).
6. A. Oren, Prokaryote diversity and taxonomy: current status and future challenges. *Philosophical Transactions of the Royal Society B-Biological Sciences* **359**, 623-638 (2004).
7. W. B. Whitman, D. C. Coleman, W. J. Wiebe, Prokaryotes: The unseen majority. *Proceedings of the National Academy of Sciences of the United States of America* **95**, 6578-6583 (1998).
8. R. E. Blankenship, Early Evolution of Photosynthesis. *Plant Physiology* **154**, 434-438 (2010).
9. Z. Masinovsky, G. I. Lozovaya, A. A. Sivash, Some Aspects of the Early Evolution of Photosynthesis. *Life Sciences and Space Research Xxiv (3) : Planetary Biology and Origins of Life* **12**, 199-205 (1992).
10. R. R. Bartz, C. A. Piantadosi, Clinical review: Oxygen as a signaling molecule. *Critical Care* **14**, (2010).
11. N. J. Planavsky *et al.*, No evidence for high atmospheric oxygen levels 1,400 million years ago. *Proceedings of the National Academy of Sciences of the United States of America* **113**, E2550-E2551 (2016).
12. N. J. Planavsky *et al.*, Low Mid-Proterozoic atmospheric oxygen levels and the delayed rise of animals. *Science* **346**, 635-638 (2014).
13. G. T. Babcock, How oxygen is activated and reduced in respiration. *Proceedings of the National Academy of Sciences of the United States of America* **96**, 12971-12973 (1999).
14. I. Vercellino, L. A. Sazanov, The assembly, regulation and function of the mitochondrial respiratory chain. *Nature Reviews Molecular Cell Biology* **23**, 141-161 (2022).
15. W. Kuhlbrandt, Structure and function of mitochondrial membrane protein complexes. *Bmc Biology* **13**, (2015).

16. J. Raymond, D. Segre, The effect of oxygen on biochemical networks and the evolution of complex life. *Science* **311**, 1764-1767 (2006).
17. M. L. Circu, T. Y. Aw, Reactive oxygen species, cellular redox systems, and apoptosis. *Free Radic Biol Med* **48**, 749-762 (2010).
18. J. D. Crapo, Morphologic changes in pulmonary oxygen toxicity. *Annu Rev Physiol* **48**, 721-731 (1986).
19. J. S. Boden, K. O. Konhauser, L. J. Robbins, P. Sanchez-Baracaldo, Timing the evolution of antioxidant enzymes in cyanobacteria. *Nature Communications* **12**, (2021).
20. D. C. Rees, J. B. Howard, The interface between the biological and inorganic worlds: Iron-sulfur metalloclusters. *Science* **300**, 929-931 (2003).
21. F. Li, Z. Qiao, Q. Duan, E. Nevo, Adaptation of mammals to hypoxia. *Animal Model Exp Med* **4**, 311-318 (2021).
22. G. L. Semenza, Oxygen sensing, hypoxia-inducible factors, and disease pathophysiology. *Annu Rev Pathol* **9**, 47-71 (2014).
23. P. S. Chen *et al.*, Pathophysiological implications of hypoxia in human diseases. *J Biomed Sci* **27**, 63 (2020).
24. W. G. Kaelin, Jr., P. J. Ratcliffe, Oxygen sensing by metazoans: the central role of the HIF hydroxylase pathway. *Mol Cell* **30**, 393-402 (2008).
25. P. Lee, N. S. Chandel, M. C. Simon, Cellular adaptation to hypoxia through hypoxia inducible factors and beyond. *Nat Rev Mol Cell Biol* **21**, 268-283 (2020).
26. K. Saxena, M. K. Jolly, Acute vs. Chronic vs. Cyclic Hypoxia: Their Differential Dynamics, Molecular Mechanisms, and Effects on Tumor Progression. *Biomolecules* **9**, (2019).
27. G. L. Semenza, Hypoxia-inducible factors in physiology and medicine. *Cell* **148**, 399-408 (2012).
28. J. Schodel, P. J. Ratcliffe, Mechanisms of hypoxia signalling: new implications for nephrology. *Nat Rev Nephrol* **15**, 641-659 (2019).
29. S. Markolovic, S. E. Wilkins, C. J. Schofield, Protein Hydroxylation Catalyzed by 2-Oxoglutarate-dependent Oxygenases. *J Biol Chem* **290**, 20712-20722 (2015).
30. G. L. Semenza, HIF-1: mediator of physiological and pathophysiological responses to hypoxia. *J Appl Physiol (1985)* **88**, 1474-1480 (2000).
31. M. E. Pamenter, J. E. Hall, Y. Tanabe, T. S. Simonson, Cross-Species Insights Into Genomic Adaptations to Hypoxia. *Front Genet* **11**, 743 (2020).
32. G. L. Semenza *et al.*, Hypoxia response elements in the aldolase A, enolase 1, and lactate dehydrogenase A gene promoters contain essential binding sites for hypoxia-inducible factor 1. *J Biol Chem* **271**, 32529-32537 (1996).
33. M. S. Nakazawa, B. Keith, M. C. Simon, Oxygen availability and metabolic adaptations. *Nat Rev Cancer* **16**, 663-673 (2016).
34. J. W. Kim, I. Tchernyshyov, G. L. Semenza, C. V. Dang, HIF-1-mediated expression of pyruvate dehydrogenase kinase: a metabolic switch required for cellular adaptation to hypoxia. *Cell Metab* **3**, 177-185 (2006).

35. I. Papandreou, R. A. Cairns, L. Fontana, A. L. Lim, N. C. Denko, HIF-1 mediates adaptation to hypoxia by actively downregulating mitochondrial oxygen consumption. *Cell Metab* **3**, 187-197 (2006).
36. R. D. Guzy *et al.*, Mitochondrial complex III is required for hypoxia-induced ROS production and cellular oxygen sensing. *Cell Metab* **1**, 401-408 (2005).
37. J. Garcia-Bermudez *et al.*, Aspartate is a limiting metabolite for cancer cell proliferation under hypoxia and in tumours. *Nat Cell Biol* **20**, 775-781 (2018).
38. M. Aga *et al.*, Exosomal HIF1alpha supports invasive potential of nasopharyngeal carcinoma-associated LMP1-positive exosomes. *Oncogene* **33**, 4613-4622 (2014).
39. C. Shao *et al.*, Role of hypoxia-induced exosomes in tumor biology. *Mol Cancer* **17**, 120 (2018).
40. K. Nakayama, N. Kataoka, Regulation of Gene Expression under Hypoxic Conditions. *Int J Mol Sci* **20**, (2019).
41. I. H. Jain *et al.*, Genetic Screen for Cell Fitness in High or Low Oxygen Highlights Mitochondrial and Lipid Metabolism. *Cell* **181**, 716-727 e711 (2020).
42. W. Johnson, O. Onuma, M. Owolabi, S. Sachdev, Stroke: a global response is needed. *Bull World Health Organ* **94**, 634-634A (2016).
43. D. Lloyd-Jones *et al.*, Heart disease and stroke statistics--2009 update: a report from the American Heart Association Statistics Committee and Stroke Statistics Subcommittee. *Circulation* **119**, 480-486 (2009).
44. A. Di Carlo *et al.*, Frequency of stroke in Europe: A collaborative study of population-based cohorts. ILSA Working Group and the Neurologic Diseases in the Elderly Research Group. Italian Longitudinal Study on Aging. *Neurology* **54**, S28-33 (2000).
45. M. A. Moskowitz, E. H. Lo, C. Iadecola, The science of stroke: mechanisms in search of treatments. *Neuron* **67**, 181-198 (2010).
46. A. A. Baburamani, C. J. Ek, D. W. Walker, M. Castillo-Melendez, Vulnerability of the developing brain to hypoxic-ischemic damage: contribution of the cerebral vasculature to injury and repair? *Front Physiol* **3**, 424 (2012).
47. U. Bruer *et al.*, Induction of tolerance in rat cortical neurons: hypoxic preconditioning. *FEBS Lett* **414**, 117-121 (1997).
48. S. Bernardo-Castro *et al.*, Therapeutic Nanoparticles for the Different Phases of Ischemic Stroke. *Life (Basel)* **11**, (2021).
49. V. E. O'Collins *et al.*, 1,026 experimental treatments in acute stroke. *Ann Neurol* **59**, 467-477 (2006).
50. W. Hacke *et al.*, Thrombolysis with alteplase 3 to 4.5 hours after acute ischemic stroke. *N Engl J Med* **359**, 1317-1329 (2008).
51. J. Rao *et al.*, Mechanical Thrombectomy for Acute Ischemic Stroke in Patients With Cardiac Myxoma: A Case Series and Pooled Analysis. *Front Neurol* **13**, 877056 (2022).
52. J. N. Cobley, M. L. Fiorello, D. M. Bailey, 13 reasons why the brain is susceptible to oxidative stress. *Redox Biol* **15**, 490-503 (2018).

53. W. Abdullahi, D. Tripathi, P. T. Ronaldson, Blood-brain barrier dysfunction in ischemic stroke: targeting tight junctions and transporters for vascular protection. *Am J Physiol Cell Physiol* **315**, C343-C356 (2018).
54. K. P. Doyle, R. P. Simon, M. P. Stenzel-Poore, Mechanisms of ischemic brain damage. *Neuropharmacology* **55**, 310-318 (2008).
55. M. Ankarcrona *et al.*, Glutamate-induced neuronal death: a succession of necrosis or apoptosis depending on mitochondrial function. *Neuron* **15**, 961-973 (1995).
56. R. Daneman, The blood-brain barrier in health and disease. *Ann Neurol* **72**, 648-672 (2012).
57. B. V. Zlokovic, The blood-brain barrier in health and chronic neurodegenerative disorders. *Neuron* **57**, 178-201 (2008).
58. D. Chappell *et al.*, Antithrombin reduces shedding of the endothelial glycocalyx following ischaemia/reperfusion. *Cardiovasc Res* **83**, 388-396 (2009).
59. K. Nian, I. C. Harding, I. M. Herman, E. E. Ebong, Blood-Brain Barrier Damage in Ischemic Stroke and Its Regulation by Endothelial Mechanotransduction. *Front Physiol* **11**, 605398 (2020).
60. L. L. Latour, D. W. Kang, M. A. Ezzeddine, J. A. Chalela, S. Warach, Early blood-brain barrier disruption in human focal brain ischemia. *Ann Neurol* **56**, 468-477 (2004).
61. R. Prakash, S. T. Carmichael, Blood-brain barrier breakdown and neovascularization processes after stroke and traumatic brain injury. *Curr Opin Neurol* **28**, 556-564 (2015).
62. Z. Merali, K. Huang, D. Mikulis, F. Silver, A. Kassner, Evolution of blood-brain-barrier permeability after acute ischemic stroke. *PLoS One* **12**, e0171558 (2017).
63. D. Strbian *et al.*, The blood-brain barrier is continuously open for several weeks following transient focal cerebral ischemia. *Neuroscience* **153**, 175-181 (2008).
64. S. P. Gadani, J. T. Walsh, J. R. Lukens, J. Kipnis, Dealing with Danger in the CNS: The Response of the Immune System to Injury. *Neuron* **87**, 47-62 (2015).
65. T. Shichita *et al.*, MAFB prevents excess inflammation after ischemic stroke by accelerating clearance of damage signals through MSR1. *Nat Med* **23**, 723-732 (2017).
66. C. Xing, K. Arai, E. H. Lo, M. Hommel, Pathophysiologic cascades in ischemic stroke. *Int J Stroke* **7**, 378-385 (2012).
67. K. Shi *et al.*, Global brain inflammation in stroke. *Lancet Neurol* **18**, 1058-1066 (2019).
68. H. C. Abeysinghe, E. L. Phillips, H. Chin-Cheng, P. M. Beart, C. L. Roulston, Modulating Astrocyte Transition after Stroke to Promote Brain Rescue and Functional Recovery: Emerging Targets Include Rho Kinase. *Int J Mol Sci* **17**, 288 (2016).
69. J. Astrup, B. K. Siesjo, L. Symon, Thresholds in cerebral ischemia - the ischemic penumbra. *Stroke* **12**, 723-725 (1981).
70. J. Liu *et al.*, Vascular remodeling after ischemic stroke: mechanisms and therapeutic potentials. *Prog Neurobiol* **115**, 138-156 (2014).

71. M. Pekna, M. Pekny, M. Nilsson, Modulation of neural plasticity as a basis for stroke rehabilitation. *Stroke* **43**, 2819-2828 (2012).
72. M. Hatakeyama, I. Ninomiya, M. Kanazawa, Angiogenesis and neuronal remodeling after ischemic stroke. *Neural Regen Res* **15**, 16-19 (2020).
73. J. R. Pan *et al.*, Hypoxic tissues are associated with microvessel density following brain ischemia-reperfusion. *Neurol Sci* **31**, 765-771 (2010).
74. H. Zhu *et al.*, Inflammation-Mediated Angiogenesis in Ischemic Stroke. *Front Cell Neurosci* **15**, 652647 (2021).
75. G. J. del Zoppo, T. Mabuchi, Cerebral microvessel responses to focal ischemia. *J Cereb Blood Flow Metab* **23**, 879-894 (2003).
76. J. Krupinski, J. Kaluza, P. Kumar, S. Kumar, J. M. Wang, Role of angiogenesis in patients with cerebral ischemic stroke. *Stroke* **25**, 1794-1798 (1994).
77. J. Adamczak, M. Hoehn, Poststroke angiogenesis, con: dark side of angiogenesis. *Stroke* **46**, e103-104 (2015).
78. Y. Fan, G. Y. Yang, Therapeutic angiogenesis for brain ischemia: a brief review. *J Neuroimmune Pharmacol* **2**, 284-289 (2007).
79. F. Fernandez-Klett, J. Priller, The fibrotic scar in neurological disorders. *Brain Pathol* **24**, 404-413 (2014).
80. I. B. Wanner *et al.*, Glial scar borders are formed by newly proliferated, elongated astrocytes that interact to corral inflammatory and fibrotic cells via STAT3-dependent mechanisms after spinal cord injury. *J Neurosci* **33**, 12870-12886 (2013).
81. D. Z. Wang, J. A. Rose, D. S. Honings, D. J. Garwacki, J. C. Milbrandt, Treating acute stroke patients with intravenous tPA. The OSF stroke network experience. *Stroke* **31**, 77-81 (2000).
82. Y. Huang, S. Chen, Y. Luo, Z. Han, Crosstalk between Inflammation and the BBB in Stroke. *Curr Neuropharmacol* **18**, 1227-1236 (2020).
83. P. Ehrlich, *Das Sauerstoff-Bedürfniss des Organismus*. (A.Hirschwald, Berlin, 1885).
84. T. S. Reese, M. J. Karnovsky, Fine structural localization of a blood-brain barrier to exogenous peroxidase. *J Cell Biol* **34**, 207-217 (1967).
85. R. Daneman, A. Prat, The blood-brain barrier. *Cold Spring Harb Perspect Biol* **7**, a020412 (2015).
86. F. Dyrna, S. Hanske, M. Krueger, I. Bechmann, The blood-brain barrier. *J Neuroimmune Pharmacol* **8**, 763-773 (2013).
87. L. W. Lau, R. Cua, M. B. Keough, S. Haylock-Jacobs, V. W. Yong, Pathophysiology of the brain extracellular matrix: a new target for remyelination. *Nat Rev Neurosci* **14**, 722-729 (2013).
88. A. Birbrair, Pericyte Biology: Development, Homeostasis, and Disease. *Adv Exp Med Biol* **1109**, 1-3 (2018).
89. A. Krogh, The supply of oxygen to the tissues and the regulation of the capillary circulation. *J Physiol* **52**, 457-474 (1919).

90. M. D. Sweeney, S. Ayyadurai, B. V. Zlokovic, Pericytes of the neurovascular unit: key functions and signaling pathways. *Nat Neurosci* **19**, 771-783 (2016).
91. R. I. Grant *et al.*, Organizational hierarchy and structural diversity of microvascular pericytes in adult mouse cortex. *J Cereb Blood Flow Metab* **39**, 411-425 (2019).
92. M. W. Majesky, Developmental basis of vascular smooth muscle diversity. *Arterioscler Thromb Vasc Biol* **27**, 1248-1258 (2007).
93. P. Dore-Duffy, Pericytes: pluripotent cells of the blood brain barrier. *Curr Pharm Des* **14**, 1581-1593 (2008).
94. A. Trost *et al.*, Brain and Retinal Pericytes: Origin, Function and Role. *Front Cell Neurosci* **10**, 20 (2016).
95. D. Virgintino *et al.*, An intimate interplay between precocious, migrating pericytes and endothelial cells governs human fetal brain angiogenesis. *Angiogenesis* **10**, 35-45 (2007).
96. G. Thanabalasundaram, C. Pieper, M. Lischper, H. J. Galla, Regulation of the blood-brain barrier integrity by pericytes via matrix metalloproteinases mediated activation of vascular endothelial growth factor in vitro. *Brain Res* **1347**, 1-10 (2010).
97. S. Watanabe *et al.*, Cultured retinal pericytes stimulate in vitro angiogenesis of endothelial cells through secretion of a fibroblast growth factor-like molecule. *Atherosclerosis* **130**, 101-107 (1997).
98. K. Y. Aguilera, R. A. Brekken, Recruitment and retention: factors that affect pericyte migration. *Cell Mol Life Sci* **71**, 299-309 (2014).
99. A. Ostman, M. Andersson, C. Betsholtz, B. Westermark, C. H. Heldin, Identification of a cell retention signal in the B-chain of platelet-derived growth factor and in the long splice version of the A-chain. *Cell Regul* **2**, 503-512 (1991).
100. P. Lindblom *et al.*, Endothelial PDGF-B retention is required for proper investment of pericytes in the microvessel wall. *Genes Dev* **17**, 1835-1840 (2003).
101. M. J. Cipolla, in *The Cerebral Circulation*. (San Rafael (CA), 2009).
102. D. Shepro, N. M. Morel, Pericyte physiology. *FASEB J* **7**, 1031-1038 (1993).
103. R. A. Caruso *et al.*, Ultrastructural descriptions of pericyte/endothelium peg-socket interdigitations in the microvasculature of human gastric carcinomas. *Anticancer Res* **29**, 449-453 (2009).
104. C. N. Duong, D. Vestweber, Mechanisms Ensuring Endothelial Junction Integrity Beyond VE-Cadherin. *Front Physiol* **11**, 519 (2020).
105. E. A. Winkler, R. D. Bell, B. V. Zlokovic, Central nervous system pericytes in health and disease. *Nat Neurosci* **14**, 1398-1405 (2011).
106. S. Tietz, B. Engelhardt, Brain barriers: Crosstalk between complex tight junctions and adherens junctions. *J Cell Biol* **209**, 493-506 (2015).
107. R. Daneman, L. Zhou, A. A. Kebede, B. A. Barres, Pericytes are required for blood-brain barrier integrity during embryogenesis. *Nature* **468**, 562-566 (2010).
108. M. W. Bobbie *et al.*, Reduced connexin 43 expression and its effect on the development of vascular lesions in retinas of diabetic mice. *Invest Ophthalmol Vis Sci* **51**, 3758-3763 (2010).

109. H. Jeon *et al.*, Pericytes from microvessel fragment produce type IV collagen and multiple laminin isoforms. *Biosci Biotechnol Biochem* **60**, 856-861 (1996).
110. A. Armulik *et al.*, Pericytes regulate the blood-brain barrier. *Nature* **468**, 557-561 (2010).
111. A. P. Sagare *et al.*, Pericyte loss influences Alzheimer-like neurodegeneration in mice. *Nat Commun* **4**, 2932 (2013).
112. E. D. Gomes *et al.*, Co-Transplantation of Adipose Tissue-Derived Stromal Cells and Olfactory Ensheathing Cells for Spinal Cord Injury Repair. *Stem Cells* **36**, 696-708 (2018).
113. F. G. Teixeira *et al.*, Impact of the Secretome of Human Mesenchymal Stem Cells on Brain Structure and Animal Behavior in a Rat Model of Parkinson's Disease. *Stem Cells Transl Med* **6**, 634-646 (2017).
114. A. Gaceb, M. Barbariga, I. Ozen, G. Paul, The pericyte secretome: Potential impact on regeneration. *Biochimie* **155**, 16-25 (2018).
115. A. Gaceb, G. Paul, Pericyte Secretome. *Adv Exp Med Biol* **1109**, 139-163 (2018).
116. J. Rustenhoven, D. Jansson, L. C. Smyth, M. Dragunow, Brain Pericytes As Mediators of Neuroinflammation. *Trends Pharmacol Sci* **38**, 291-304 (2017).
117. F. Shimizu *et al.*, Peripheral nerve pericytes modify the blood-nerve barrier function and tight junctional molecules through the secretion of various soluble factors. *J Cell Physiol* **226**, 255-266 (2011).
118. A. Gaceb, I. Ozen, T. Padel, M. Barbariga, G. Paul, Pericytes secrete pro-regenerative molecules in response to platelet-derived growth factor-BB. *J Cereb Blood Flow Metab* **38**, 45-57 (2018).
119. X. Yuan *et al.*, Exosomes Derived From Pericytes Improve Microcirculation and Protect Blood-Spinal Cord Barrier After Spinal Cord Injury in Mice. *Front Neurosci* **13**, 319 (2019).
120. G. van Niel, G. D'Angelo, G. Raposo, Shedding light on the cell biology of extracellular vesicles. *Nat Rev Mol Cell Biol* **19**, 213-228 (2018).
121. R. Kalluri, V. S. LeBleu, The biology, function, and biomedical applications of exosomes. *Science* **367**, (2020).
122. G. J. del Zoppo, G. W. Schmid-Schonbein, E. Mori, B. R. Copeland, C. M. Chang, Polymorphonuclear leukocytes occlude capillaries following middle cerebral artery occlusion and reperfusion in baboons. *Stroke* **22**, 1276-1283 (1991).
123. J. R. Little, F. W. Kerr, T. M. Sundt, Jr., Microcirculatory obstruction in focal cerebral ischemia. Relationship to neuronal alterations. *Mayo Clin Proc* **50**, 264-270 (1975).
124. J. R. Little, F. W. Kerr, T. M. Sundt, Jr., Microcirculatory Obstruction in Focal Cerebral Ischemia: An Electron Microscopic Investigation in Monkeys. *Stroke* **7**, 25-30 (1976).
125. M. Yemisci *et al.*, Pericyte contraction induced by oxidative-nitrative stress impairs capillary reflow despite successful opening of an occluded cerebral artery. *Nat Med* **15**, 1031-1037 (2009).

126. C. N. Hall *et al.*, Capillary pericytes regulate cerebral blood flow in health and disease. *Nature* **508**, 55-60 (2014).
127. M. Kang, Y. Yao, Basement Membrane Changes in Ischemic Stroke. *Stroke* **51**, 1344-1352 (2020).
128. R. G. Underly *et al.*, Pericytes as Inducers of Rapid, Matrix Metalloproteinase-9-Dependent Capillary Damage during Ischemia. *J Neurosci* **37**, 129-140 (2017).
129. H. Jiao, Z. Wang, Y. Liu, P. Wang, Y. Xue, Specific role of tight junction proteins claudin-5, occludin, and ZO-1 of the blood-brain barrier in a focal cerebral ischemic insult. *J Mol Neurosci* **44**, 130-139 (2011).
130. B. Duz, E. Oztas, T. Erginay, E. Erdogan, E. Gonul, The effect of moderate hypothermia in acute ischemic stroke on pericyte migration: an ultrastructural study. *Cryobiology* **55**, 279-284 (2007).
131. E. Gonul *et al.*, Early pericyte response to brain hypoxia in cats: an ultrastructural study. *Microvasc Res* **64**, 116-119 (2002).
132. S. Y. Zhou, Z. N. Guo, D. H. Zhang, Y. Qu, H. Jin, The Role of Pericytes in Ischemic Stroke: Fom Cellular Functions to Therapeutic Targets. *Front Mol Neurosci* **15**, 866700 (2022).
133. I. Ozen *et al.*, Brain pericytes acquire a microglial phenotype after stroke. *Acta Neuropathol* **128**, 381-396 (2014).
134. I. Masuho *et al.*, A Global Map of G Protein Signaling Regulation by RGS Proteins. *Cell* **183**, 503-521 e519 (2020).
135. R. Ganss, Keeping the Balance Right: Regulator of G Protein Signaling 5 in Vascular Physiology and Pathology. *Prog Mol Biol Transl Sci* **133**, 93-121 (2015).
136. C. Bondjers *et al.*, Transcription profiling of platelet-derived growth factor-B-deficient mouse embryos identifies RGS5 as a novel marker for pericytes and vascular smooth muscle cells. *Am J Pathol* **162**, 721-729 (2003).
137. H. Cho, T. Kozasa, C. Bondjers, C. Betsholtz, J. H. Kehrl, Pericyte-specific expression of Rgs5: implications for PDGF and EDG receptor signaling during vascular maturation. *FASEB J* **17**, 440-442 (2003).
138. J. Hamzah *et al.*, Vascular normalization in Rgs5-deficient tumours promotes immune destruction. *Nature* **453**, 410-414 (2008).
139. Y. Jin *et al.*, RGS5, a hypoxia-inducible apoptotic stimulator in endothelial cells. *J Biol Chem* **284**, 23436-23443 (2009).
140. M. J. Lee *et al.*, Characterization of arginylation branch of N-end rule pathway in G-protein-mediated proliferation and signaling of cardiomyocytes. *J Biol Chem* **287**, 24043-24052 (2012).
141. M. J. Lee *et al.*, RGS4 and RGS5 are in vivo substrates of the N-end rule pathway. *Proc Natl Acad Sci U S A* **102**, 15030-15035 (2005).
142. N. Masson *et al.*, Conserved N-terminal cysteine dioxygenases transduce responses to hypoxia in animals and plants. *Science* **365**, 65-69 (2019).
143. J. J. Gunaje, A. J. Bahrami, S. M. Schwartz, G. Daum, W. M. Mahoney, Jr., PDGF-dependent regulation of regulator of G protein signaling-5 expression and vascular smooth muscle cell functionality. *Am J Physiol Cell Physiol* **301**, C478-489 (2011).

144. J. Zhou *et al.*, Characterization of RGS5 in regulation of G protein-coupled receptor signaling. *Life Sci* **68**, 1457-1469 (2001).
145. L. Huang *et al.*, Glial scar formation occurs in the human brain after ischemic stroke. *Int J Med Sci* **11**, 344-348 (2014).
146. S. Lively, I. Moxon-Emre, L. C. Schlichter, SC1/hevin and reactive gliosis after transient ischemic stroke in young and aged rats. *J Neuropathol Exp Neurol* **70**, 913-929 (2011).
147. D. O. Dias, C. Goritz, Fibrotic scarring following lesions to the central nervous system. *Matrix Biol* **68-69**, 561-570 (2018).
148. F. Fernandez-Klett *et al.*, Early loss of pericytes and perivascular stromal cell-induced scar formation after stroke. *J Cereb Blood Flow Metab* **33**, 428-439 (2013).
149. N. Makihara *et al.*, Involvement of platelet-derived growth factor receptor beta in fibrosis through extracellular matrix protein production after ischemic stroke. *Exp Neurol* **264**, 127-134 (2015).
150. E. H. Lo, A new penumbra: transitioning from injury into repair after stroke. *Nat Med* **14**, 497-500 (2008).
151. E. H. Lo, Experimental models, neurovascular mechanisms and translational issues in stroke research. *Br J Pharmacol* **153 Suppl 1**, S396-405 (2008).
152. A. Asgari Taei *et al.*, Enhancement of angiogenesis and neurogenesis by intracerebroventricular injection of secretome from human embryonic stem cell-derived mesenchymal stem cells in ischemic stroke model. *Biomed Pharmacother* **140**, 111709 (2021).
153. C. J. Cunningham, E. Redondo-Castro, S. M. Allan, The therapeutic potential of the mesenchymal stem cell secretome in ischaemic stroke. *J Cereb Blood Flow Metab* **38**, 1276-1292 (2018).
154. R. A. Loiola *et al.*, Secretome of endothelial progenitor cells from stroke patients promotes endothelial barrier tightness and protects against hypoxia-induced vascular leakage. *Stem Cell Res Ther* **12**, 552 (2021).
155. H. Takagi, G. L. King, G. S. Robinson, N. Ferrara, L. P. Aiello, Adenosine mediates hypoxic induction of vascular endothelial growth factor in retinal pericytes and endothelial cells. *Invest Ophthalmol Vis Sci* **37**, 2165-2176 (1996).
156. S. Wakui *et al.*, Localization of Ang-1, -2, Tie-2, and VEGF expression at endothelial-pericyte interdigitation in rat angiogenesis. *Lab Invest* **86**, 1172-1184 (2006).
157. K. Ishitsuka *et al.*, Neurotrophin production in brain pericytes during hypoxia: a role of pericytes for neuroprotection. *Microvasc Res* **83**, 352-359 (2012).
158. I. Guijarro-Munoz, M. Compte, A. Alvarez-Cienfuegos, L. Alvarez-Vallina, L. Sanz, Lipopolysaccharide activates Toll-like receptor 4 (TLR4)-mediated NF-kappaB signaling pathway and proinflammatory response in human pericytes. *J Biol Chem* **289**, 2457-2468 (2014).
159. C. Pieper, J. J. Marek, M. Unterberg, T. Schwerdtle, H. J. Galla, Brain capillary pericytes contribute to the immune defense in response to cytokines or LPS in vitro. *Brain Res* **1550**, 1-8 (2014).

160. C. Pieper, P. Pieloch, H. J. Galla, Pericytes support neutrophil transmigration via interleukin-8 across a porcine co-culture model of the blood-brain barrier. *Brain Res* **1524**, 1-11 (2013).
161. J. Rustenhoven *et al.*, TGF-beta1 regulates human brain pericyte inflammatory processes involved in neurovasculature function. *J Neuroinflammation* **13**, 37 (2016).
162. Q. Wu *et al.*, Differential miRNA expression analysis of extracellular vesicles from brain microvascular pericytes in spontaneous hypertensive rats. *Biotechnol Lett* **42**, 389-401 (2020).
163. E. L. A. S, I. Mager, X. O. Breakefield, M. J. Wood, Extracellular vesicles: biology and emerging therapeutic opportunities. *Nat Rev Drug Discov* **12**, 347-357 (2013).
164. D. Athauda *et al.*, Utility of Neuronal-Derived Exosomes to Examine Molecular Mechanisms That Affect Motor Function in Patients With Parkinson Disease: A Secondary Analysis of the Exenatide-PD Trial. *JAMA Neurol* **76**, 420-429 (2019).
165. B. Wang *et al.*, Circulating microparticles in patients after ischemic stroke: a systematic review and meta-analysis. *Rev Neurosci*, (2018).
166. J. B. Williams, E. C. Jauch, C. J. Lindsell, B. Campos, Endothelial microparticle levels are similar in acute ischemic stroke and stroke mimics due to activation and not apoptosis/necrosis. *Acad Emerg Med* **14**, 685-690 (2007).
167. M. Vanlandewijck *et al.*, A molecular atlas of cell types and zonation in the brain vasculature. *Nature* **554**, 475-480 (2018).
168. P. Androvic *et al.*, Decoding the Transcriptional Response to Ischemic Stroke in Young and Aged Mouse Brain. *Cell Rep* **31**, 107777 (2020).
169. L. V. Dergunova *et al.*, Genome-wide transcriptome analysis using RNA-Seq reveals a large number of differentially expressed genes in a transient MCAO rat model. *BMC Genomics* **19**, 655 (2018).
170. R. I. Kestner *et al.*, Gene Expression Dynamics at the Neurovascular Unit During Early Regeneration After Cerebral Ischemia/Reperfusion Injury in Mice. *Front Neurosci* **14**, 280 (2020).
171. K. Guo *et al.*, Single-Cell RNA Sequencing With Combined Use of Bulk RNA Sequencing to Reveal Cell Heterogeneity and Molecular Changes at Acute Stage of Ischemic Stroke in Mouse Cortex Penumbra Area. *Front Cell Dev Biol* **9**, 624711 (2021).
172. K. Zheng *et al.*, Single-cell RNA-seq reveals the transcriptional landscape in ischemic stroke. *J Cereb Blood Flow Metab* **42**, 56-73 (2022).
173. F. Takata *et al.*, Oncostatin M-induced blood-brain barrier impairment is due to prolonged activation of STAT3 signaling in vitro. *J Cell Biochem* **119**, 9055-9063 (2018).
174. C. Yu *et al.*, Syndecan-1 Facilitates the Human Mesenchymal Stem Cell Osteo-Adipogenic Balance. *Int J Mol Sci* **21**, (2020).
175. M. H. Nisancioglu *et al.*, Generation and characterization of rgs5 mutant mice. *Mol Cell Biol* **28**, 2324-2331 (2008).
176. G. Llovera, S. Roth, N. Plesnila, R. Veltkamp, A. Liesz, Modeling stroke in mice: permanent coagulation of the distal middle cerebral artery. *J Vis Exp*, e51729 (2014).

177. J. Chang *et al.*, Gpr124 is essential for blood-brain barrier integrity in central nervous system disease. *Nat Med* **23**, 450-460 (2017).
178. O. Jacobson, D. O. Kiesewetter, X. Chen, Albumin-Binding Evans Blue Derivatives for Diagnostic Imaging and Production of Long-Acting Therapeutics. *Bioconjug Chem* **27**, 2239-2247 (2016).
179. M. R. Rafiee *et al.*, Protease-resistant streptavidin for interaction proteomics. *Mol Syst Biol* **16**, e9370 (2020).
180. K. F. Cho *et al.*, Proximity labeling in mammalian cells with TurboID and split-TurboID. *Nat Protoc* **15**, 3971-3999 (2020).
181. I. Ozen *et al.*, Loss of Regulator of G-Protein Signaling 5 Leads to Neurovascular Protection in Stroke. *Stroke* **49**, 2182-2190 (2018).
182. O. Renner *et al.*, Time- and cell type-specific induction of platelet-derived growth factor receptor-beta during cerebral ischemia. *Brain Res Mol Brain Res* **113**, 44-51 (2003).
183. W. Wei *et al.*, Cell type-selective secretome profiling in vivo. *Nat Chem Biol* **17**, 326-334 (2021).
184. S. Schafer *et al.*, IL-11 is a crucial determinant of cardiovascular fibrosis. *Nature* **552**, 110-115 (2017).
185. A. A. Widjaja *et al.*, Inhibiting Interleukin 11 Signaling Reduces Hepatocyte Death and Liver Fibrosis, Inflammation, and Steatosis in Mouse Models of Nonalcoholic Steatohepatitis. *Gastroenterology* **157**, 777-792 e714 (2019).
186. S. Dasgupta *et al.*, RGS5-TGFbeta-Smad2/3 axis switches pro- to anti-apoptotic signaling in tumor-residing pericytes, assisting tumor growth. *Cell Death Differ* **28**, 3052-3076 (2021).
187. W. M. Mahoney, Jr., J. Gunaje, G. Daum, X. R. Dong, M. W. Majesky, Regulator of G-protein signaling - 5 (RGS5) is a novel repressor of hedgehog signaling. *PLoS One* **8**, e61421 (2013).
188. C. Xu, Y. M. Li, B. Sun, F. J. Zhong, L. Y. Yang, ATE1 Inhibits Liver Cancer Progression through RGS5-Mediated Suppression of Wnt/beta-Catenin Signaling. *Mol Cancer Res* **19**, 1441-1453 (2021).
189. M. M. Brandt *et al.*, Transcriptome analysis reveals microvascular endothelial cell-dependent pericyte differentiation. *Sci Rep* **9**, 15586 (2019).
190. M. Hellstrom *et al.*, Lack of pericytes leads to endothelial hyperplasia and abnormal vascular morphogenesis. *J Cell Biol* **153**, 543-553 (2001).
191. Y. Chen, G. Li, M. L. Liu, Microvesicles as Emerging Biomarkers and Therapeutic Targets in Cardiometabolic Diseases. *Genomics Proteomics Bioinformatics* **16**, 50-62 (2018).
192. M. Yanez-Mo *et al.*, Biological properties of extracellular vesicles and their physiological functions. *J Extracell Vesicles* **4**, 27066 (2015).
193. H. B. B, N. Akhtar, A. Alrohimi, K. Khan, A. Shuaib, Stroke mimics: incidence, aetiology, clinical features and treatment. *Ann Med* **53**, 420-436 (2021).
194. B. Zhang *et al.*, Interleukin-11 treatment protected against cerebral ischemia/reperfusion injury. *Biomed Pharmacother* **115**, 108816 (2019).

Acknowledgements

Expressing the depth of gratitude, I have for the numerous people who have supported and contributed to my journey in completing this thesis is no easy feat.

First and foremost, I would like to express my deepest gratitude to my supervisor Professor Gesine Paul-Visse. Thank you for your invaluable guidance, encouragement, and support throughout this entire process. Your expertise, passion for science, and hard work is truly admirable and working with you has been a great privilege. You have always valued my opinions and ideas and given me the freedom to pursue my own research questions and at the same time given me honest and essential feedback when needed.

To my co-supervisors Robert Carlsson and Anja Meissner. Robert, your unique perspectives, expertise, and insights have helped me to improve my research in so many ways. Thank you for being my sounding board and for always being willing to grab a coffee whenever I have questions, whether they be related to the intricacies of science or the complexities of life. I consider you not only a great mentor, but also a friend and for that I am truly grateful! To Anja, thank you for always being encouraging and supportive whenever I have needed it.

A special thank you to all past and present members of the TNY group. Without your contributions, completing this thesis would have been a lot harder. To Ilknur, thank you for taking me under your wings and introducing me to the world of pericytes; Osama, thank you for your kind heart and always being encouraging; Abderahim, for always providing valuable feedback; Michaela; for your contagious laughter and bringing the sunshine into the office; Carolina, thank you for always spreading positivity around the office, all the extensive proof reading, and introducing me to culinary alternatives besides stamstället.

I have crossed paths with so many wonderful and interesting people during my PhD! To all my fellow PhD students and colleagues at different corners of BMC, I am grateful for the camaraderie, shared experiences and support that we have given each other over the years. I would like to extend a special thank you to all of you at A10 for contributing to a welcoming, stimulating, and collaborative environment where everyone is always willing to lend a helping hand. You have all made my time here so much more fulfilling.

Life can get hectic sometimes and it is reassuring to have great friends to keep one's own sanity intact. To my friends 'near and far', thank you for contributing to that and so much more! And know that my absence of late does not reflect my love and appreciation I have for all of you.

It is hard to put into words how lucky I feel to have such a wonderful family. To my dear parents, thank you for your unwavering support and guidance, for creating a loving home and the warmest of upbringings, and for being inspiring role models who have taught me so much in life. To my sister Fanny, thank you for being my confidante, for sharing my humour, and for your big heart. To my aunt Ylva, thank you for your constant support, for your wise counsel, for your generosity, and for bringing me along on sailing and skiing adventures.

Daniela, you bring so much light into my life! Thank you for always being there for me, for always being honest and speaking your mind, for your kindness, and for making me laugh. I am so incredibly grateful to have meet you and I am filled with excitement to see what the future holds for the two of us.

Lastly, thank you for guitars and padel rackets, you have been a constant source of stress relief.

Printed by Media-Tryck, Lund 2023 NORDIC SWAN ECOLABEL 3041 0903

About the author

Andreas Enström has previously studied Molecular Biology in Lund. He joined the Translational Neurology group in 2019 under the supervision of Gesine Paul-Visse. Andreas has explored different aspects of how pericytes respond to ischemic stroke and how that affects the pathological progression. On the 11th of May 2023, Andreas will defend his thesis entitled "Pericytes in Hypoxia and Ischemic Stroke", in Segerfalksalen, Wallenberg Neuroscience Center Lund University.

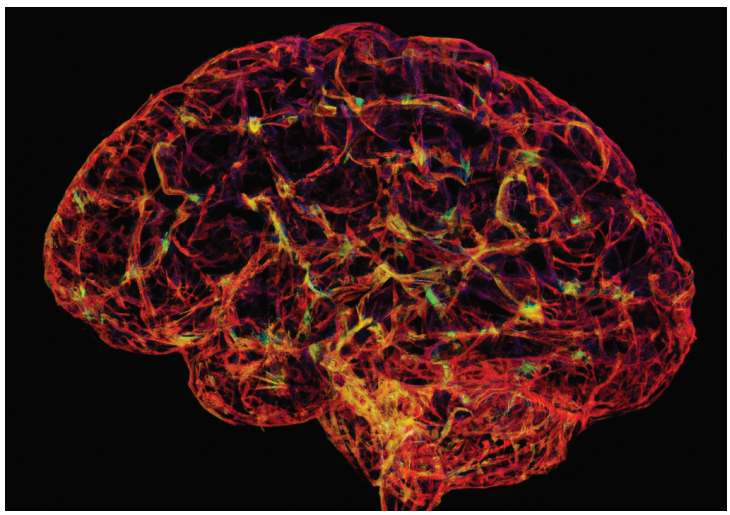

LUND UNIVERSITY

FACULTY OF MEDICINE

Department of Clinical Sciences

Lund University, Faculty of Medicine
Doctoral Dissertation Series 2023:62
ISBN 978-91-8021-402-5
ISSN 1652-8220